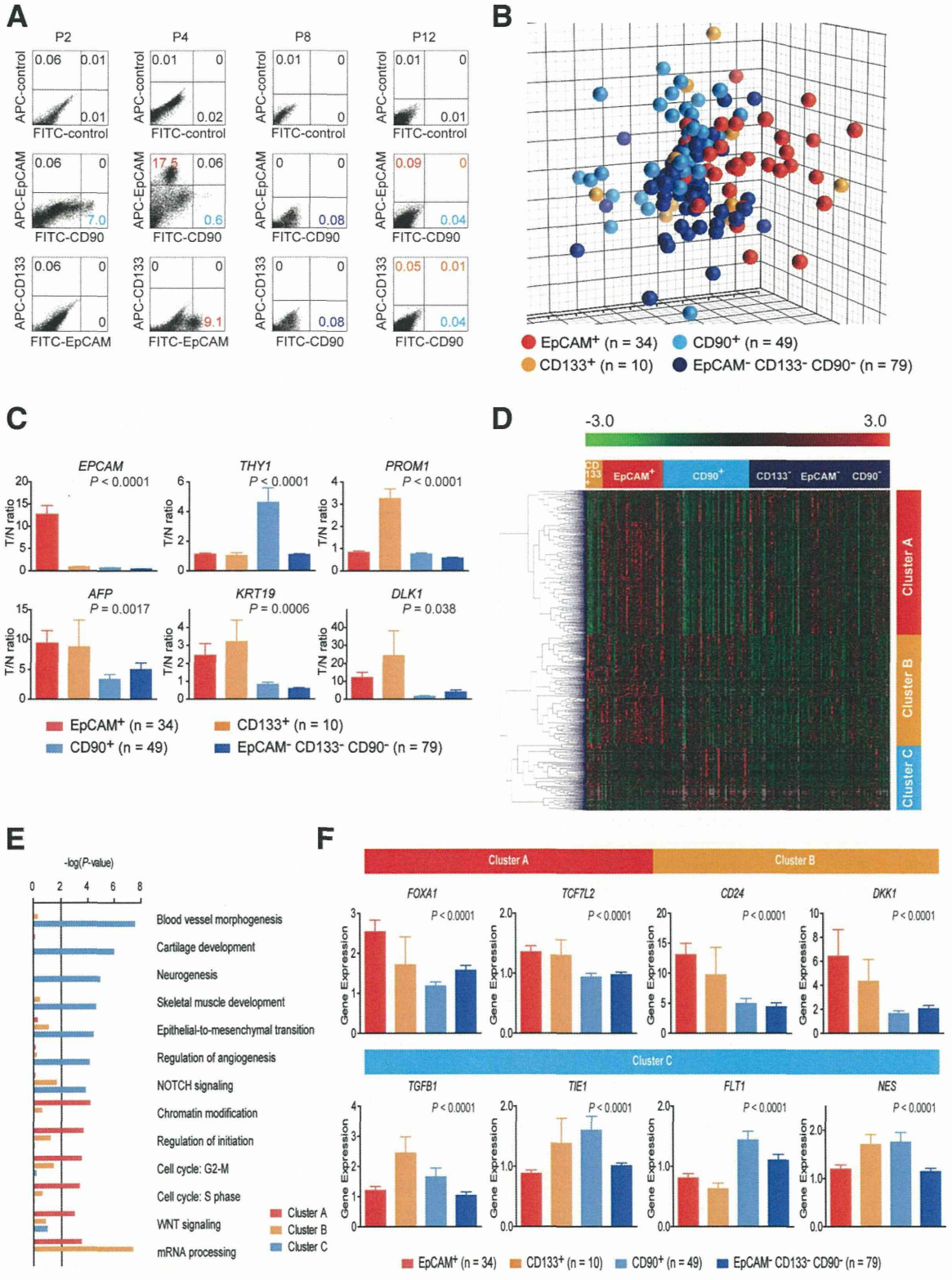

Fig. 1. Gene-expression profiles of CSC marker-positive HCCs. (A) FACS analysis of primary HCCs stained with fluorescent-labeled Abs against EpCAM, CD90, or CD133. (B) Multidimensional scaling analysis of 172 HCC cases characterized by the expression patterns of EpCAM, CD133, and CD90. Red, $EpCAM^+$ $CD90^-$ $CD133^-$ ($n = 34$); orange, $EpCAM^-$ $CD90^-$ $CD133^+$ ($n = 10$); light blue, $EpCAM^-$ $CD90^+$ $CD133^-$ ($n = 49$); blue, $EpCAM^-$ $CD90^-$ $CD133^-$ ($n = 79$). HCC specimens were clustered in specific groups with statistical significance ($P < 0.001$). (C) Expression patterns of well-known hepatic stem/progenitor markers in each HCC subtype, as analyzed by microarray. Red bar, $EpCAM^+$; orange bar, $CD133^+$; light blue bar, $CD90^+$; blue bar, $EpCAM^-$ $CD90^-$ $CD133^-$. (D) Hierarchical cluster analysis based on 1,561 EpCAM/CD90/CD133-coregulated genes in 172 HCC cases. Each cell in the matrix represents the expression level of a gene in an individual sample. Red and green cells depict high and low expression levels, respectively, as indicated by the scale bar. (E) Pathway analysis of EpCAM/CD90/CD133-coregulated genes. Canonical signaling pathways activated in cluster A (red bar), cluster B (orange bar), or cluster C (light blue bar) with statistical significance ($P < 0.01$) are shown. (F) Expression patterns of representative genes differentially expressed in EpCAM/CD90/CD133 HCC subtypes. Red bar, $EpCAM^+$; orange bar, $CD133^+$; light blue bar, $CD90^+$; blue bar, $EpCAM^-$ $CD133^-$ $CD90^-$.

Table 2. Tumorigenic Capacity of Unsorted, EpCAM$^+$, EpCAM$^-$, CD90$^+$, and CD90$^-$ Cells From Primary HCCs and Xenografts

Sample	CD133 (%)	CD90 (%)	EpCAM (%)	Cell Surface Marker	Number of Cells	Tumor Formation 2M	Tumor Formation 3M
P1	0	3.1	0	Unsorted	1×10^7	0/5	0/5
				CD90$^+$	1×10^5	0/5	0/5
				CD90$^-$	1×10^5	0/5	0/5
P2	0.06	7.0	0.06	Unsorted	1×10^7	0/5	0/5
				CD90$^+$	1×10^5	0/5	0/5
				CD90$^-$	1×10^5	0/5	0/5
P3	0	1.3	0	Unsorted	1×10^6	0/2	0/2
				CD90$^+$	1×10^4	0/4	0/4
				CD90$^-$	1×10^4	0/4	0/4
P4	0	0.6	17.5	Unsorted	1×10^6	3/4	4/4
				EpCAM$^+$	1×10^3	0/3	2/3
					1×10^4	3/4	4/4
					1×10^5	3/3	3/3
				CD90$^+$	1×10^3	0/3	0/3
					1×10^4	0/4	0/4
					1×10^5	0/3	0/3
				EpCAM$^-$ CD90$^-$	1×10^3	0/3	0/3
					1×10^4	0/4	0/4
					1×10^5	0/3	0/3
P5	0	0.8	29.7	Unsorted	1×10^6	0/5	0/5
				EpCAM$^+$	1×10^5	0/5	0/5
				CD90$^+$	1×10^5	0/5	0/5
				EpCAM$^-$ CD90$^-$	1×10^5	0/5	0/5
P6	0	0.7	0	Unsorted	1×10^6	0/2	0/2
				CD90$^+$	1×10^4	0/4	0/4
				CD90$^-$	1×10^4	0/4	0/4
P7	1.38	4.5	4.4	Unsorted	1×10^6	2/2	2/2
				EpCAM$^+$	2×10^2	0/3	0/3
					1×10^3	0/3	1/3
					1×10^4	2/4	4/4
				CD90$^+$	2×10^2	0/3	0/3
					1×10^3	0/3	0/3
					1×10^4	0/4	0/4
				EpCAM$^-$ CD90$^-$	1×10^3	0/3	0/3
					1×10^4	0/3	0/3
					1×10^5	0/4	0/4
P8	0	0.08	0	Unsorted	1×10^5	0/4	0/4
				CD90$^+$	1×10^3	0/3	0/3
				CD90$^-$	1×10^5	0/3	0/3
P9	0	0.26	0	Unsorted	1×10^5	0/4	0/4
				CD90$^+$	1×10^3	0/3	0/3
				CD90$^-$	1×10^5	0/3	0/3
P10	0	0.78	0	Unsorted	1×10^4	0/4	0/4
				CD90$^+$	1×10^3	0/3	0/3
				CD90$^-$	1×10^4	0/3	0/3
P11	0	0.1	1.54	Unsorted	5×10^4	0/2	0/2
				EpCAM$^+$	1×10^3	0/3	0/3
				CD90$^+$	1×10^3	0/3	0/3
				EpCAM$^-$ CD90$^-$	1×10^4	0/3	0/3
P12	0.06	0.05	0.09	Unsorted	1×10^5	0/3	3/3
				CD90$^+$	1×10^3	0/4	1/4
				CD90$^-$	1×10^3	0/4	1/4
					1×10^4	0/3	3/3
P13	0	0.03	67.7	EpCAM$^+$	5×10^5	4/4	NA
					5×10^4	3/3	NA
					5×10^3	3/3	NA
				EpCAM$^-$	5×10^5	0/4	NA
					5×10^4	0/3	NA
					5×10^3	0/3	NA
P14	24.0	0.06	3.1	EpCAM$^+$	5×10^3	4/5	NA
				EpCAM$^-$	5×10^3	2/5	NA
P15	0	2.45	0	CD90$^+$	5×10^4	3/4	NA
					5×10^3	1/3	NA
					5×10^2	1/3	NA
				CD90$^-$	5×10^4	2/4	NA
					5×10^3	1/3	NA
					5×10^2	0/3	NA

NA, not available.

contained definite CD133$^+$ cells (20%) (Table 2). CD90$^+$ cells were detected at variable frequencies in all 15 HCCs analyzed.

To explore the status of these CSC marker-positive cells in HCC in a large cohort, we utilized oligo-DNA microarray data from 238 HCC cases (GEO accession no.: GSE5975) to evaluate the expression of *EPCAM* (encoding EpCAM and CD326), *THY1* (encoding CD90), and *PROM1* (encoding CD133) in whole HCC tissues and nontumor (NT) tissues. Because previous studies demonstrated that CD133$^+$ and CD90$^+$ cells were detected at low frequency (~13.6% by CD133 staining and ~6.2% by CD90 staining) in HCC, but were almost nonexistent in NT liver (4, 5),[4,5] we utilized tumor/nontumor (T/N) gene-expression ratios to detect the existence of marker-positive CSCs in tumor. Accordingly, we showed that a 2-fold cutoff of T/N ratios of *EPCAM* successfully stratifies HCC samples with EpCAM$^+$ liver CSCs.[9,10]

A total of 95 (39.9%), 110 (46.2%), and 31 (13.0%) of the 238 HCC cases were thus regarded as EpCAM$^+$, CD90$^+$, and CD133$^+$ HCCs (T/N ratios: $\geq$2.0), respectively. As observed in the FACS data described above, we detected coexpression of EpCAM and CD90 in 45 HCCs (18.9%), EpCAM and CD133 in five HCCs (2%), CD90 and CD133 in five HCCs (2%), and EpCAM, CD90, and CD133 in 11 HCCs (4.6%). To clarify the characteristics of gene-expression signatures specific to stem cell marker expression status, we selected 172 HCC cases expressing a single CSC marker (34 EpCAM$^+$ CD90$^-$ CD133$^-$, 49 EpCAM$^-$ CD90$^+$ CD133$^-$, and 10 EpCAM$^-$ CD90$^-$ CD133$^+$) or all marker-negative HCCs (79 EpCAM$^-$ CD90$^-$ CD133$^-$). A class-comparison analysis with

univariate F tests and a global permutation test (×10,000) yielded a total of 1,561 differentially expressed genes. Multidimensional scaling (MDS) analysis using this gene set indicated that HCC specimens were clustered in specific groups with statistical significance ($P < 0.001$). Close examination of MDS plots revealed three major HCC subtype clusters: all marker-negative HCCs (blue spheres); EpCAM single-positive HCCs (red spheres); and CD90 single-positive HCCs (light blue spheres). $CD133^+$ HCCs (orange spheres) were rare, relatively scattered, and not clustered (Fig. 1B).

We examined the expression of representative hepatic stem/progenitor cell markers *AFP*, *KRT19*, and *DLK1* in HCCs with regard to the gene-expression status of each CSC marker (Fig. 1C). All three markers were up-regulated in $EpCAM^+$ and $CD133^+$ HCCs, compared with all marker-negative HCCs, consistent with previous findings.[10,11] However, we found no significant overexpression of *AFP*, *KRT19*, and *DLK1* in $CD90^+$ and all marker-negative HCCs.

Hierarchical cluster analyses revealed three main gene clusters that were up-regulated in $EpCAM^+$ HCCs (cluster A, 706 genes), $EpCAM^+$ or $CD133^+$ HCCs (cluster B, 530 genes), and $CD90^+$ or $CD133^+$ HCCs (cluster C, 325 genes) (Fig. 1D). Pathway analysis indicated that the enriched genes in cluster A (red bar) were associated with chromatin modification, cell-cycle regulation, and Wnt/β-catenin signaling (Fig. 1E). Genes associated with messenger RNA processing were enriched in clusters A (red bar) and B (orange bar). Surprisingly, genes in cluster C were significantly associated with pathways involved in blood-vessel morphogenesis, angiogenesis, neurogenesis, and epithelial mesenchymal transition (EMT) (light blue bar). Close examination of genes in each cluster suggested that known hepatic transcription factors (*FOXA1*), Wnt regulators (*TCF7L2* and *DKK1*), and a hepatic stem cell marker (*CD24*) were dominantly up-regulated in $EpCAM^+$ and $CD133^+$ HCCs (Fig. 1F). By contrast, genes associated with blood-vessel morphogenesis (*TIE1* and *FLT1*), EMT (*TGFB1*), and neurogenesis (*NES*) were activated dominantly in $CD90^+$ HCCs and $CD133^+$ HCCs.

$CD90^+$ HCC Cells Share Features With Mesenchymal Vascular Endothelial Cells. Because $CD133^+$ HCCs were relatively rare and constituted only 13% (microarray cohort) to 20% (FACS cohort) of all HCC samples analyzed, we focused on the characterization of EpCAM and CD90. To clarify the cell identity of $EpCAM^+$ or $CD90^+$ cells in primary HCCs, we performed IHC analysis of 18 needle-biopsy specimens of premalignant dysplastic nodules (DNs), 102 surgically resected HCCs, and corresponding NT liver tissues. When examining the expression of EpCAM and CD90 in cirrhotic liver tissue by double-color IHC analysis, we found that $EpCAM^+$ cells and $CD90^+$ cells were distinctively located and not colocalized (Supporting Fig. 1A). Immunoreactivity (IR) to anti-CD90 antibodies (Abs) was detected in vascular endothelial cells (VECs), inflammatory cells, fibroblasts, and neurons, but not in hepatocytes or cholangiocytes, in the cirrhotic liver (Supporting Fig. 1B, panels a,b). IR to anti-EpCAM Abs was detected in hepatic progenitors adjacent to the periportal area and bile duct epithelial cells in liver cirrhosis (Supporting Fig. 1B, panels c,d).

IR to anti-EpCAM Abs was detected in 37 of 102 surgically resected HCCs (Fig. 2A, panel b), but not in 18 DNs (Fig. 2A, panel a). By contrast, no tumor epithelial cells (TECs) showing IR to anti-CD90 Abs were found in any of the 18 DNs or 102 HCCs examined (Fig. 2A, panels c,d). However, we identified $CD90^+$ cells that were morphologically similar to VECs or fibroblasts within the tumor nodule in 37 of the 102 surgically resected HCC tissues (≥5% positive staining in a given area). IR to anti-CD90 Abs was also detected in hepatic mesenchymal tumors (Supporting Fig. 1C, panels a-c), indicating that CD90 is also a marker of liver stromal tumors.

Double-color IHC and immunofluorescence (IF) analysis confirmed the distinct expression of EpCAM and CD90 in HCC (Fig. 2B), consistent with the FACS data (Fig. 1A). Quantitative real-time polymerase chain reaction (qPCR) analysis of sorted $EpCAM^+$, $CD90^+$, and $EpCAM^-$ $CD90^-$ cells after $CD45^+$ cell depletion indicated that the hepatic stem/progenitor markers, *AFP* and *KRT19*, were up-regulated in $EpCAM^+$ cells (red bar), whereas the mesenchymal markers, *KIT* and *FLT1*, were up-regulated in $CD90^+$ cells (orange bar), compared with $EpCAM^-$ $CD90^-$ cells (blue bar) (Fig. 2C). The hepatocyte marker, *CYP3A4*, was down-regulated in $EpCAM^+$ cells and not detected in $CD90^+$ cells, compared with $EpCAM^-$ $CD90^-$ cells. *POU5F1* and *BMI1* were equally up-regulated in both $EpCAM^+$ and $CD90^+$ cells, compared with $EpCAM^-$ $CD90^-$ cells.

EpCAM and CD90 were independently and distinctively expressed in different cellular lineages, so we evaluated the staining of EpCAM and CD90 separately and analyzed the clinicopathological characteristics of surgically resected HCC cases. HCCs were regarded marker positive if ≥5% positive staining was detected in a given area. The existence of $EpCAM^+$

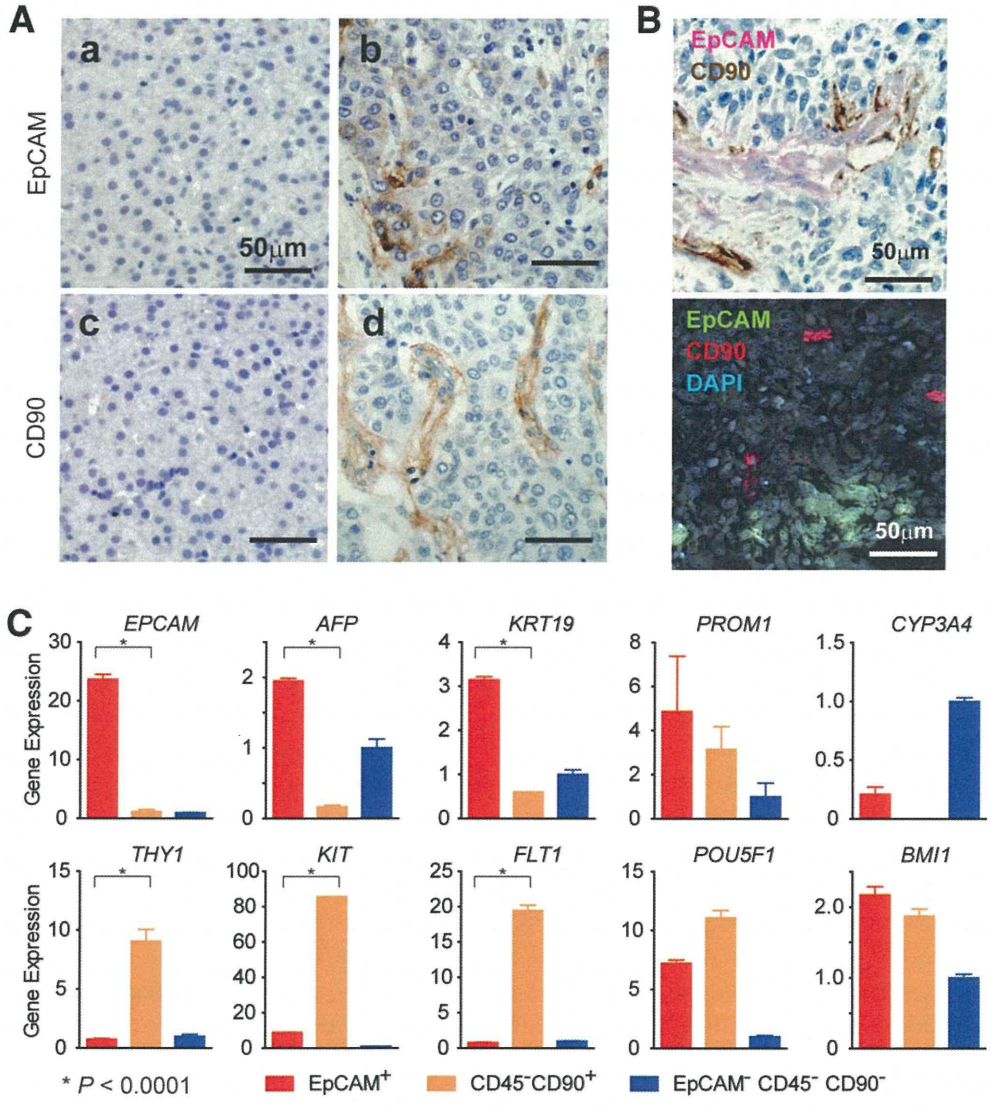

Fig. 2. Distinct EpCAM$^+$ and CD90$^+$ cell populations in HCC. (A) Representative images of EpCAM and CD90 staining in dysplastic nodule (panels a,c) and HCC (panels b,d) by IHC analysis (scale bar, 50 μm). EpCAM (panels a,b) and CD90 (panels c,d) immunostaining is depicted. (B) Upper panel: representative images of EpCAM (red) and CD90 (brown) double staining in HCC by IHC (scale bar, 50 μm). Lower panel: representative images of EpCAM (green) and CD90 (red) staining with 4'6-diamidino-phenylindole (DAPI) (blue) in HCC by IF (scale bar, 50 μm). (C) qPCR analysis of sorted EpCAM$^+$ (red bar), CD90$^+$ (orange bar), or EpCAM$^-$ CD90$^-$ (blue bar) derived from a representative primary HCC. Experiments were performed in triplicate, and data are shown as mean ± standard error of the mean.

cells (≥5%) was characterized by poorly differentiated morphology and high serum AFP values with a tendency for portal vein invasion, whereas the existence of CD90$^+$ cells (≥5%) was associated with poorly differentiated morphology and a tendency for large tumor size (Supporting Tables 2 and 3). Notably, the existence of CD90$^+$ cells was associated with a high incidence of distant organ metastasis, including lung, bone, and adrenal gland, within 2 years after surgery, whereas EpCAM$^+$ cell abundance appeared unrelated to distant organ metastasis.

We evaluated the characteristics of EpCAM$^+$ or CD90$^+$ cells in seven representative HCC cell lines. Morphologically, all EpCAM$^+$ cell lines (HuH1, HuH7, and Hep3B) showed a polygonal, epithelial cell shape, whereas three of four CD90$^+$ cell lines (HLE, HLF, and SK-Hep-1) showed a spindle cell shape (Fig. 3A). EpCAM$^+$ cells were detected in 11.5%, 57.7%, and 99.6% of sorted HuH1, HuH7, and Hep3B cells, respectively. A small CD90$^+$ cell population (0.66%) was observed in PLC/PRL/5, whereas 91.3%, 10.8%, and 59.0% of CD90$^+$ cells were detected in HLE, HLF, and SK-Hep-1, respectively. Compared with primary HCCs, only EpCAM$^+$ or CD90$^+$ cells were detected in liver cancer cell lines under normal culture conditions (Fig. 3B), suggesting that these cell lines contain a relatively pure cell population most likely obtained by clonal selection through the establishment process.

A class-comparison analysis with univariate t tests and a global permutation test (×10,000) of microarray data yielded two main gene clusters up-regulated in EpCAM$^+$ cell lines (HuH1, HuH7, and Hep3B) (cluster I, 524 genes) or in CD90$^+$ cell lines (HLE, HLF, and SK-Hep-1) (cluster II, 366 genes) (Fig. 3C). PLC/PRL/5 showed intermediate gene-expression patterns between EpCAM$^+$ and CD90$^+$ cell lines using this gene set. Pathway analysis indicated that the genes

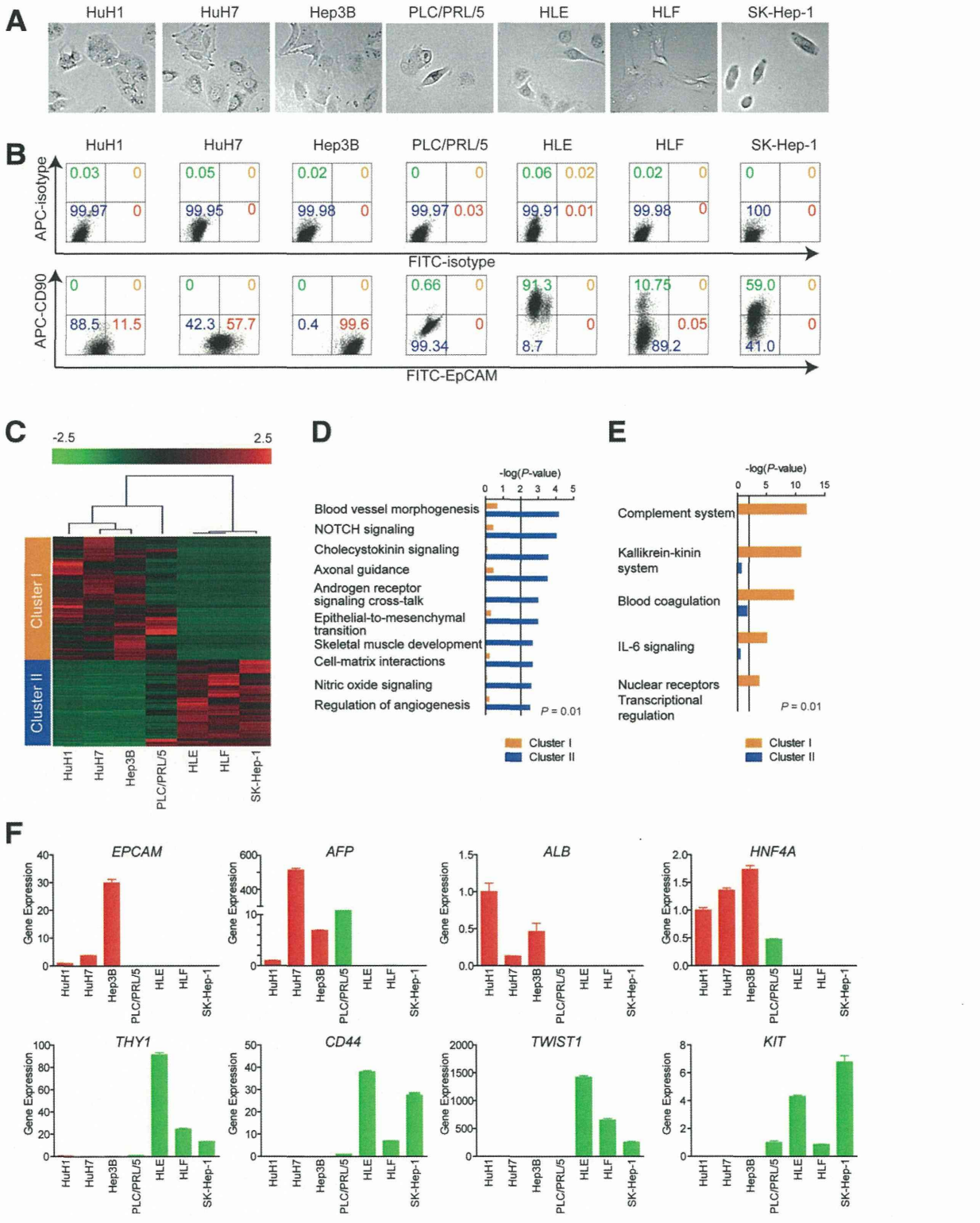

Fig. 3. Characteristics of HCC cell lines defined by EpCAM and CD90. (A) Representative photomicrographs of $EpCAM^{+}CD90^{-}$ and $EpCAM^{-}CD90^{+}$ HCC cell lines. (B) Representative FACS data of $EpCAM^{+}CD90^{-}$ and $EpCAM^{-}CD90^{+}$ HCC cell lines stained with fluorescein isothiocyanate (FITC)-EpCAM and APC-CD90 Abs. (C) Heat-map images of seven HCC cell lines based on 890 EpCAM/CD90-coregulated genes. Each cell in the matrix represents the expression level of a gene in an individual sample. Red and green cells depict high and low expression levels, respectively, as indicated by the scale bar. (D and E) Pathway analysis of EpCAM/CD90-coregulated genes. Canonical signaling pathways activated in cluster I (orange bar) or II (blue bar) with statistical significance ($P < 0.01$) are shown. (F) qPCR of representative differentially expressed genes identified by microarray analysis (C) in seven HCC cell lines.

enriched in cluster II were mainly associated with blood-vessel morpho- and angiogenesis (Fig. 3D). By contrast, the enriched genes in cluster I were significantly associated with known hepatocyte functions ($P < 0.01$) (Fig. 3E). In addition, we identified that the enriched genes in cluster II were significantly associated with neurogenesis, skeletal muscle development, and EMT.

We used qPCR to validate that known hepatic stem cell (HSC) and hepatocyte markers, such as *AFP, EPCAM, ALB*, and *HNF4A* genes, were up-regulated in $EpCAM^+$ cell lines, but not detected in $CD90^+$ cell lines (Fig. 3F). By contrast, genes associated with mesenchymal lineages and EMT, such as *KIT, TWIST1, CD44*, and *THY1*, were strongly up-regulated in $CD90^+$ cell lines.

Unique Tumorigenicity and Metastasis Capacity of Distinct CSCs Defined by EpCAM and CD90. We investigated the tumorigenic capacity of $EpCAM^+$ or $CD90^+$ cells by subcutaneously (SC) injecting 1×10^5 sorted cells of four HCC cell lines (HuH1, HuH7, HLE, and HLF) into nonobese diabetic, severe combined immunodeficient (NOD/SCID) mice. We excluded Hep3B cells for the evaluation of tumorigenicity because almost 100% of cells were EpCAM positive. We further excluded SK-Hep-1 cells from the analysis because they potentially originated from endothelial cells.[12] The highly tumorigenic capacities of $EpCAM^+$ and $CD90^+$ cells were reproduced in HuH1, HuH7, and HLF cell lines, compared with marker-negative cells (Fig. 4A). However, HLE cells did not produce SC tumors, even 12 months after transplantation, in NOD/SCID mice. $EpCAM^+$ cells from HuH1 and HuH7 formed larger tumors more rapidly than $CD90^+$ cells from HLF (Fig. 4B). IHC analyses indicated that $EpCAM^+$ cells did not produce $CD90^+$ cells and *vice versa* in these cell lines *in vivo* (Fig. 4C). $CD90^+$ cells showed a high metastatic capacity, whereas $EpCAM^+$ cells showed no metastasis to the lung when SC tumor volume reached approximately 2,000 (HuH1 and HuH7) or 700 mm^3 (HLF) (Fig. 4D). The high metastatic capacity of PLC/PRL/5 cells, which contain a small population of $CD90^+$ cells, was also confirmed after SC injection into NOD/SCID mice (data not shown). $CD90^+$ cells could divide to generate both $CD90^+$ and $CD90^-$ cells, and $CD90^+$ cells showed a high capacity to invade and form spheroids with overexpression of *TWIST1* and *TWIST2*, which are known to activate EMT programs in HLF cells (Supporting Fig. 2A-D).

We next evaluated the tumorigenic/metastatic capacity of $CD45^-$ tumor cells using 12 fresh primary HCC specimens (P1-P12) that had been surgically resected (Table 2). We further evaluated the tumorigenicity of EpCAM/CD90 sorted cells obtained from xenografts derived from primary HCCs (Supporting Fig. 3A). Of these, we confirmed the tumorigenicity of cancer cells obtained from six primary HCCs after SC injection into NOD/SCID mice within 3 months after transplantation (Fig. 5A; Table 2; Supporting Fig. 3B). $EpCAM^+$ cells derived from four HCCs (P4, P7, P13, and P14) showed highly tumorigenic capacities, compared with $EpCAM^-$ cells. $CD90^+$ cells derived from two HCCs showed equal (P12) or more-tumorigenic capacities (P15), compared with $CD90^-$ cells. Tumorigenicity of $EpCAM^+$ cells was observed in three hepatitis C virus (HCV)-related HCCs and an hepatitis B virus (HBV)-related HCC, whereas tumorigenicity of $CD90^+$ cells was observed in two HBV-related HCCs (Tables 1 and 2).

Using unsorted cells, we compared the frequency of $EpCAM^+$ and $CD90^+$ cells in primary and xenograft tumors and found that $EpCAM^+$ cells remained, but $CD90^+$ cells disappeared, in secondary tumors derived from P4 or P7, whereas $EpCAM^+$ cells disappeared, but $CD90^+$ cells remained, in secondary tumors derived from P12 (Fig. 5B). Morphologically, tumorigenic $EpCAM^+$ cells showed an epithelial cell shape, whereas $CD90^+$ cells showed a mesenchymal VEC shape (Fig. 5C and Supporting Fig. 3C). FACS analysis indicated that P12 HCC cells showed abundant expression of vascular endothelial growth factor receptor (VEGFR) 1 and a vascular endothelial marker endoglin (CD105) (Fig. 5D). By contrast, P4 and P7 HCC cells did not express these vascular endothelial markers (data not shown). Lung metastasis was detected in NOD/SCID mice transplanted with P12 HCC cells, but not in mice transplanted with P4 and P7 HCC cells (Fig. 5E,F).

Taken together, these results suggest that the tumorigenic and metastatic capability of primary HCC may depend on the presence of distinct $EpCAM^+$ or $CD90^+$ CSCs. $EpCAM^+$ cells were associated with a high tumorigenic capacity with hepatic epithelial stem cell features, whereas $CD90^+$ cells were related to the metastatic propensity with VEC features.

Suppression of Lung Metastasis Mediated by $CD90^+$ CSCs by Imatinib Mesylate. We previously demonstrated that Wnt/β-catenin signaling inhibitors could successfully attenuate the tumorigenic capacity of $EpCAM^+$ CSCs in HCC.[8,10] To explore the potential molecular targets activated in $CD90^+$ CSCs, we investigated the expression of the known VEC markers, CD105, VEGFR1 (encoded by *FLT1*), and

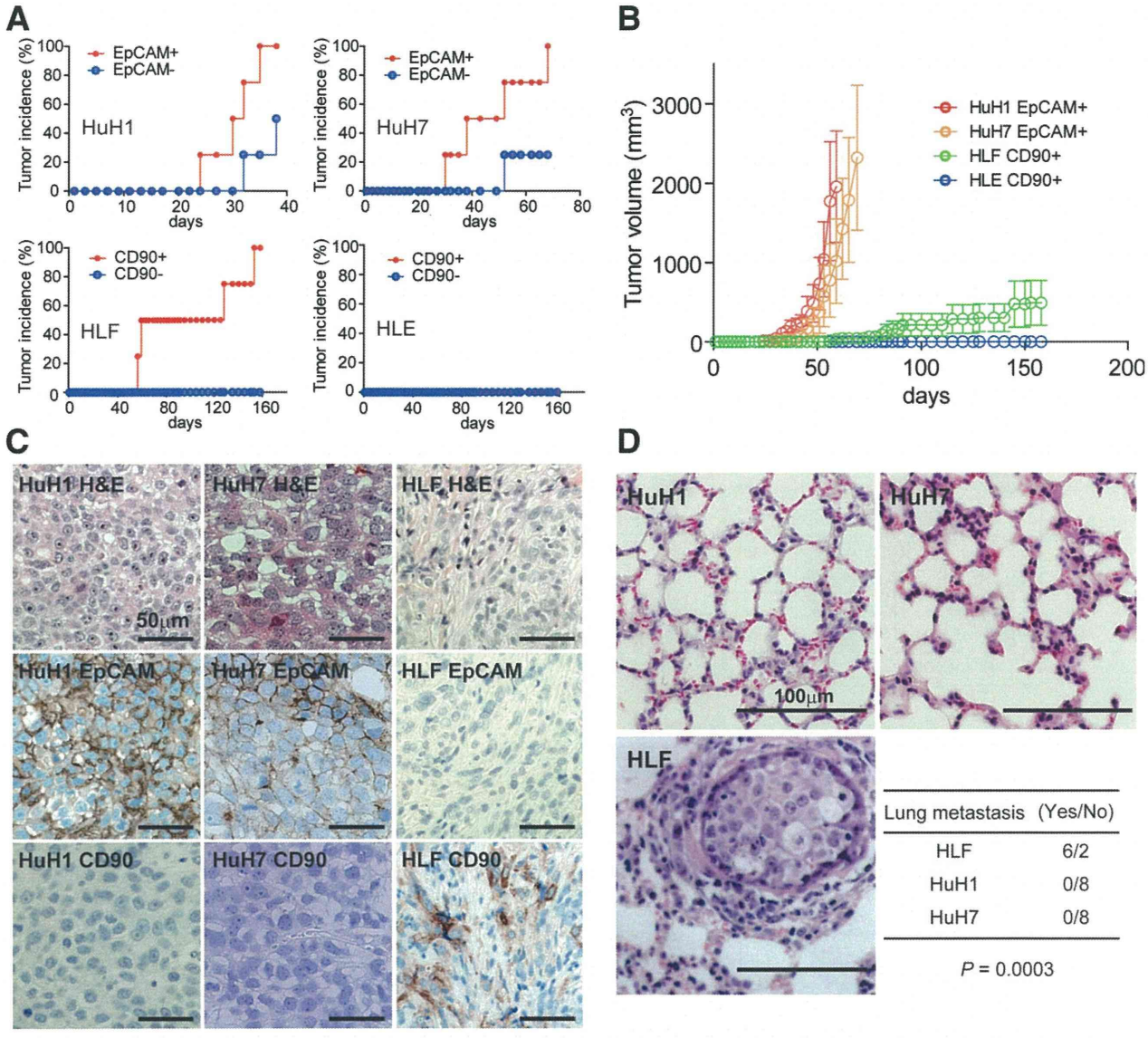

Fig. 4. Distinct tumorigenic/metastatic capacities of HCC cell lines defined by EpCAM and CD90. (A) Tumorigenicity of 1×10^5 cells sorted by anti-EpCAM (HuH1 and HuH7) or anti-CD90 (HLE and HLF) Abs. Data are generated from 8 mice/cell line. (B) Tumorigenic ability of $EpCAM^+$ and $CD90^+$ sorted cells in NOD/SCID mice. Aggressive tumor growth in the SC lesion was observed in $EpCAM^+$ HuH1 or HuH7 cells, compared with $CD90^+$ HLE or HLF cells. $EpCAM^+$ (1×10^5) or $CD90^+$ cells were injected. Tumor-volume curves are depicted as mean ± standard deviation of 4 mice/group. (C) Histological analysis of $EpCAM^+$ or $CD90^+$ cell-derived xenografts. Hematoxylin and eosin (H&E) staining of a SC tumor (upper panels) and IHC of the tumor with anti-EpCAM (middle panels) or anti-CD90 Abs (bottom panels) are shown (scale bar, 50 μm). (D) Metastasis was evaluated macroscopically and microscopically in the left and right lobes of the lung separately in each mouse (n = 4) (scale bar, 100 μm).

c-Kit (encoded by *KIT*), in cell lines and showed that they were abundantly expressed in $CD90^+$ cell lines, but not $EpCAM^+$ cell lines (Fig. 6A). No expression of VEGFR2 was detected in this set of cell lines, suggesting that molecular reagents specifically targeting VEGFR2 may have no effects on $CD90^+$ CSCs. CD44, a stem cell marker that functionally regulates redox status and is a potential target of $CD90^+$ CSCs, was also abundantly expressed in $CD90^+$ cell lines (Supporting Fig. 4A), consistent with previous data.[5,13] No significant difference was detected in the expression of the hematopoietic marker, CD34, or ABCG2 between $EpCAM^+$ and $CD90^+$ cell lines (Supporting Fig. 4A).

Among these molecular targets, we focused on the characterization of c-Kit because the c-Kit tyrosine kinase inhibitor, imatinib mesylate, is readily available, is widely used for the treatment of gastrointestinal stromal tumor with activation of c-Kit, and may have potential antitumor activity against a subset of HCC.[14] We explored the effect of imatinib mesylate on HCC cell lines and found that treatment with 10

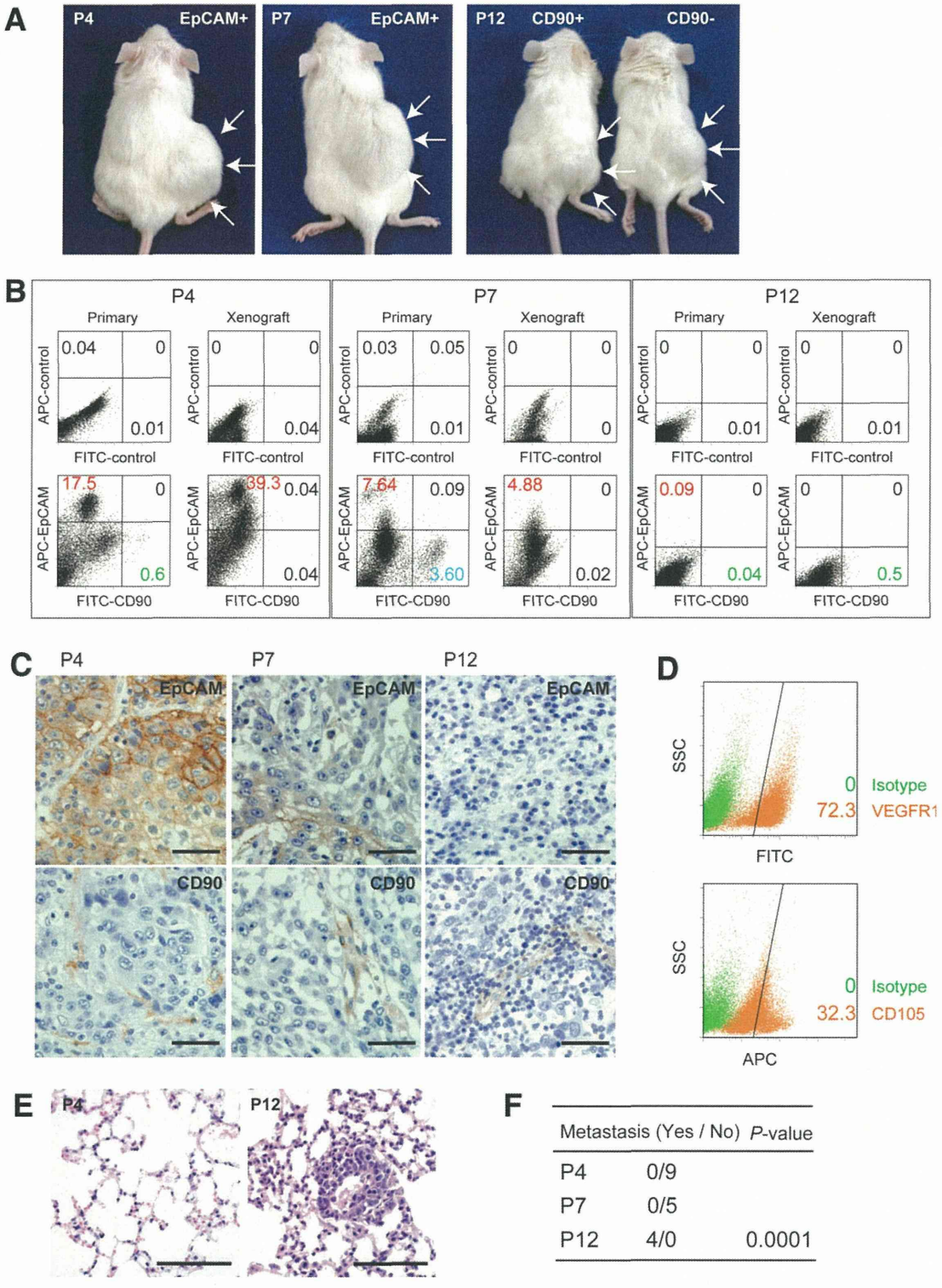

Fig. 5. Tumorigenic/metastatic capacities of EpCAM$^+$ and CD90$^+$ cells in primary HCC. (A) Representative NOD/SCID mice with SC tumors (white arrows) from EpCAM$^+$ P4 or P7 cells (left and middle panels) and CD90$^+$ or CD90$^-$ P12 cells (right panel). (B) FACS analysis of CD90 and EpCAM staining in primary HCCs and the corresponding secondary tumors developed in NOD/SCID mice. Unsorted cells (1×10^6 cells in P4 and P7 or 1×10^5 cells in P12) were SC injected to evaluate the frequency of each marker-positive cell in primary and secondary tumors. (C) IHC analysis of EpCAM and CD90 in primary HCCs P4, P7, and P12 (scale bar, 50 μm). (D) FACS analysis of VEGFR1 (Alexa488) and CD105 (APC) in primary HCC P12. (E) Hematoxylin and eosin staining of lung tissues in P4 and P12 (scale bar, 200 μm). (F) Frequency of lung metastasis in NOD/SCID mice SC transplanted using unsorted primary HCC cells.

μM reduced cell proliferation and spheroid formation in CD90$^+$ cell lines, but had no effect on EpCAM$^+$ cell lines (Supporting Fig. S4B,C).

We further explored the effect of imatinib mesylate *in vivo*. Because EpCAM$^+$ and CD90$^+$ cells reside in the primary HCC, but not in established cell lines, we SC injected HuH7 and HLF cell lines to generate tumors organized by EpCAM$^+$ and CD90$^+$ CSCs. Interestingly, when HLF cells were coinjected with HuH7 cells, EpCAM$^+$ cells could metastasize to the lung, whereas

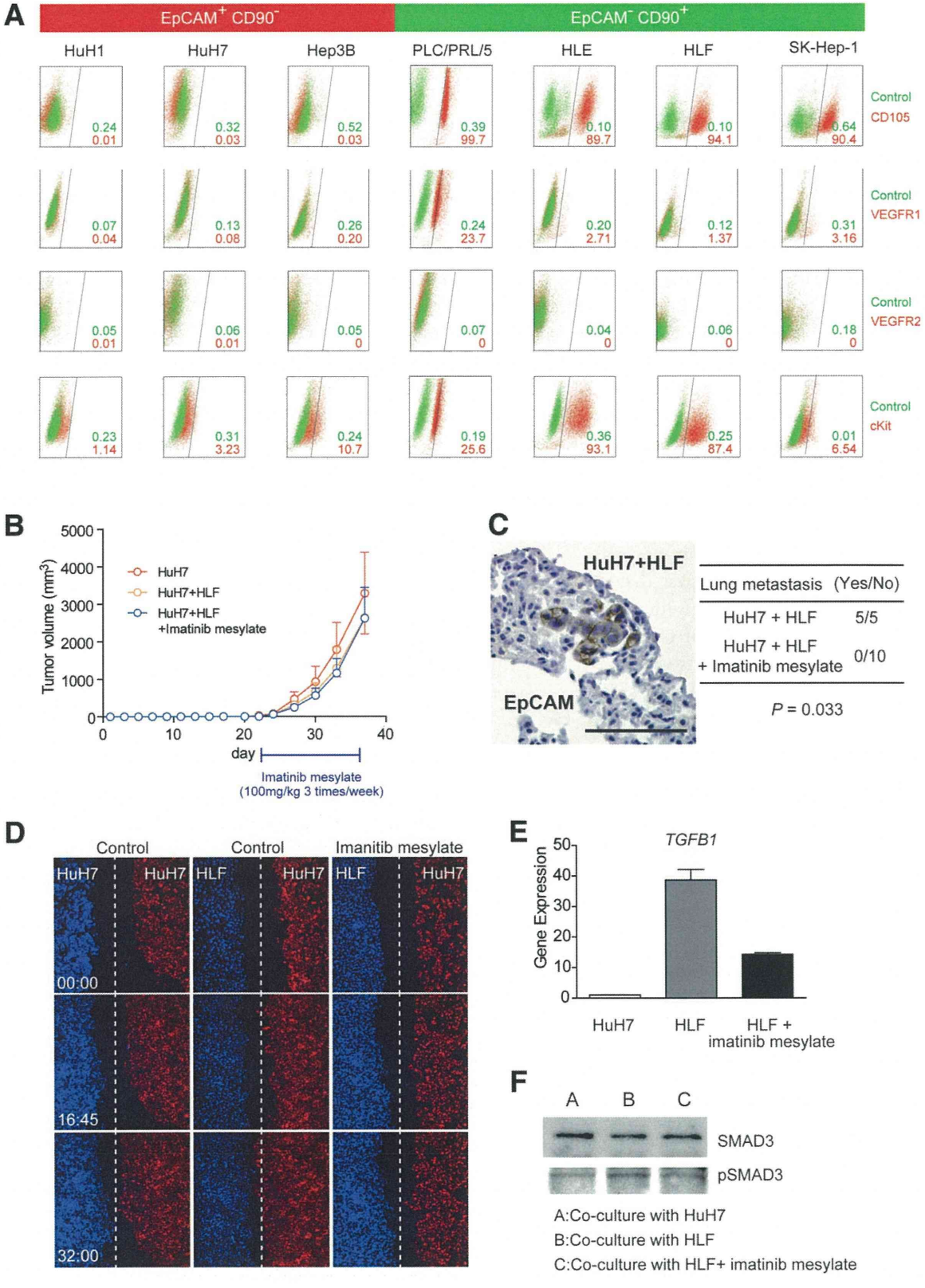

SC primary tumors showed no difference in size (Fig. 6B,C). Furthermore, although imatinib mesylate treatment had little effect on the size of primary SC tumors, it significantly suppressed lung metastasis in primary tumors (Fig. 6C). These data suggest that $CD90^+$ cells are not only metastatic to the distant organ, but also help the metastasis of $CD90^-$ cells, including $EpCAM^+$ cells, which originally have no distant metastatic capacity. Our data further suggest that imatinib mesylate can inhibit distant organ metastasis by suppressing $CD90^+$ metastatic CSCs, albeit with little effect on $EpCAM^+$ tumorigenic epithelial stem-like CSCs.

To explore the potential mechanism of how $CD90^+$ cells dictate the metastasis of $EpCAM^+$ cells, we utilized coculture systems and time-lapse image analysis. Wound-healing analysis clearly indicated that motility of HuH7 cells was enhanced when HLF cells were cocultured, and this effect was abolished by imatinib mesylate treatment (Fig. 6D; see Supporting Videos 1-3). HLF cells abundantly expressed *TGFB1*, compared with HuH7 cells, and its expression was dramatically suppressed by imatinib mesylate treatment (Fig. 6E). Mothers against decapentaplegic homolog 3 (Smad3) phosphorylation was augmented in HuH7 cells when cocultured with HLF cells, and this effect was attenuated when cocultured with HLF cells pretreated with imatinib mesylate.

Taken together, our data suggest that liver CSCs are not a single entity. Liver CSCs defined by different markers show unique features of tumorigenicity/metastasis with phenotypes closely associated with committed liver lineages. These distinct CSCs may collaborate to enhance tumorigenicity and metastasis of HCCs.

Discussion

The current investigation demonstrates that CSC marker expression status may be a key determinant of cancer phenotypes, in terms of metastatic propensity and chemosensitivity, to certain molecularly targeted therapies. EpCAM appears to be an epithelial tumorigenic CSC marker, whereas CD90 seems to be a mesenchymal metastatic CSC marker associated with expression of c-Kit and chemosensitivity to imatinib mesylate. Imatinib mesylate may be effective in inhibiting metastasis, but has little effect on primary $EpCAM^+$ HCC cell growth.

We investigated the frequency of three CSC markers (EpCAM, CD90, and CD133) in 15 primary HCCs with a confirmed cell viability of $\geq$70% and found that three HCCs contained $CD133^+$ cells, seven HCCs contained $EpCAM^+$ cells, and all HCCs contained $CD90^+$ cells. Among them, we confirmed the perpetuation of $CD133^+$ cells derived from three HCCs (P7, P12, and P14; data not shown), $EpCAM^+$ cells derived from four HCCs (P4, P7, P13, and P14), and $CD90^+$ cells derived from two HCCs (P12 and P15). Recent studies showed that at least 8 of 21 HCCs (38%)[4] and 13 of 13 HCCs (100%)[5] contained tumorigenic $CD133^+$ or $CD90^+$ CSCs, respectively. Recent IHC and tissue microarray studies also demonstrated that $CD133^+$ and $CD90^+$ cells were detected in 24.8% ($\geq$1% of tumor cells) and 32.2% ($\geq$5% of tumor cells) of HCC cases examined, respectively.[15,16]

One possible explanation of the comparatively low frequency of $CD133^+$ liver CSCs identified in our study is that we used the monoclonal Ab CD133/2, whereas Ma et al. used CD133/1. Another possible explanation is the difference of etiology related to hepatocarcinogenesis. We examined tumorigenicity using 15 HCCs (five HBV related, four HCV related, three non-B, non-C hepatitis [NBNC] related, and three alcohol related) and identified that tumorigenic CSCs were only obtained from HBV- or HCV-related cases. Previous liver CSC studies were performed using HBV-related HCCs,[4,5] and a recent study showed that

Fig. 6. Suppression of lung metastasis mediated by $CD90^+$ CSCs by imatinib mesylate. (A) FACS analysis of seven HCC cell lines stained by APC-CD105, Alexa 488/VEGFR1, APC/VEGFR2, and Alexa 488/c-Kit Abs or isotype control. (B) Tumorigenicity of 5×10^5 HuH7 cells and 2.5×10^5 HuH7 cells plus 2.5×10^5 HLF cells treated with imatinib mesylate or control phosphate-buffered saline (PBS) (200 μL/mouse) orally ingested three times per week (100 mg/kg) for 2 weeks. Data are generated from 5 mice per condition. (C) IHC analysis of EpCAM in lung metastasis detected in NOD/SCID mice SC injected with 2.5×10^5 HuH7 cells and 2.5×10^5 HLF cells. Metastasis was evaluated macro- and microscopically in the left and right lobes of the lung separately in each mouse ($n = 5$) (scale bar, 100 μm). (D) Cell motility of HuH7 cells cocultured with HuH7, HLF, or HLF cells with imatinib mesylate (10 μM) was monitored in a real-time manner by time-lapse image analysis. HuH7 and HLF cells were labeled with the lipophilic fluorescence tracer, DiI (indicated as red) or DiD (indicated as blue), and incubated in a μ-Slide eight-well chamber overnight. Silicone inserts were detached and the culture media replaced with Dulbecco's modified Eagle's medium containing 10% fetal bovine serum, including 0.1% dimethyl sulfoxide (DMSO) (control) or 10 μM of imatinib mesylate dissolved in DMSO (final concentration 0.1%). Immediately after the medium change, cells were cultured at 37°C in 5% CO_2 and time-lapse images were captured for 72 hours. (E) qPCR analysis of *TGFB1* in HuH7 (white bar), HLF (gray bar), and HLF cells pretreated with imatinib mesylate for 24 hours. (F) Smad3 and its phosphorylation evaluated by western blotting. HuH7 cells and HLF cells were harvested in cell culture inserts and treated with DMSO (0.1%) or imatinib mesylate (10 μM) for 24 hours. Cell culture inserts were washed with PBS, cocultured with HuH7 cells for 8 hours, and then removed. HuH7 cells were lysed using radioimmunoprecipitation assay buffer for western blotting. (A) HuH7 cells cocultured with HuH7 cells. (B) HuH7 cells cocultured with HLF cells. (C) HuH7 cells cocultured with HLF cells pretreated with imatinib mesylate.

HBV X may play a role in generating $EpCAM^+$ CSCs.[17] The role of hepatitis virus infection on the generation of CSCs is still unclear and should be clarified in future studies.

We were unable to confirm the tumorigenicity of $CD90^+$ cells in 13 of 15 HCCs, but we observed abundant $CD90^+$ cells in more-advanced HCCs by IHC (data not shown). Tumorigenic $CD90^+$ cells may emerge at a later stage of hepatocarcinogenesis, and the majority of $CD90^+$ cells in early HCCs may be cancer-associated VECs without tumorigenic capacity. Furthermore, we identified tumorigenic $CD90^+$ cells only from HBV-related HCCs, and a recent study suggested that expression of CD90 was associated with HBV infection.[16] We could not detect the small population of $CD90^+$ HuH7 and Hep3B cells reported on by Yang et al. However, because we identified a small population of $CD90^+$ HuH7 cells after treatment with 5-FU (manuscript in preparation), it is conceivable that different cellular stress statuses may explain the observed differences between our findings and those of Yang et al.

The majority of CSC markers discovered thus far are almost identical to those found in healthy tissue stem cells or embryonic stem cells. However, with regard to the liver, the characteristics of healthy hepatic stem/progenitor cells isolated using different stem cell markers are currently under investigation. A recent article examined the characteristics of $EpCAM^+$ and $CD90^+$ oval cells isolated from 2-acetylaminofluorene/partial hepatectomy or D-galactosamine-treated rats.[18] Interestingly, $EpCAM^+$ and $CD90^+$ oval cells represent two distinct populations: The former expresses classical oval cell markers, such as AFP, OV-1, and cytokeratin-19 (CK-19), whereas the latter expresses desmin and alpha smooth muscle actin, but not AFP, OV-1, or CK-19, which indicates that $CD90^+$ populations are more likely to be mesenchymal cells. Another study has demonstrated that mesenchymal cells can interact with HSCs to regulate cell-fate decision.[19] We found that $EpCAM^+$ and $CD90^+$ cells isolated from liver cancer are distinct in terms of gene- and protein-expression patterns in both primary liver cancers and cell lines. Furthermore, these distinct CSCs can interact to regulate the tumorigenicity and metastasis of HCC. Molecular characteristics of $EpCAM^+/CD90^+$ CSCs may potentially reflect the cellular context of healthy stem or progenitor cells.

Although our study strongly indicates that abundant $CD90^+$ cells in a tumor is a risk for distant metastasis in liver cancer, the cell identity and role of $CD90^+$ cells remains elusive. As our IHC, FACS, and xenotransplantation assays revealed, some $CD90^+$ cells in liver cancer may be cancer-associated VECs or fibroblasts that cannot perpetuate in the xenograft. Recent findings have suggested the importance of stromal cells in tumorigenesis and cancer metastasis,[20-22] so it is possible that these cells may help TECs invade and intravasate into blood vessels, thus playing crucial roles in metastasis.

Another possibility is that $CD90^+$ cells are cancer cells with features of fibroblasts (having undergone EMT) or VECs (having undergone vasculogenic mimicry; VM) that can invade, intravasate, and metastasize cells to distant organs. Recently, two groups reported that a subset of tumor VECs originate from glioblastoma CSCs.[23,24] We successfully confirmed the tumorigenicity and metastatic capacity of $CD90^+$ cells that were morphologically identical to VECs from primary HCCs that could perpetuate in the xenograft. However, a recent study demonstrated that $CD90^+$ HCC cells express glypican-3, a marker detected in hepatic epithelial cells.[25] Further studies are warranted to clarify the nature and role of $CD90^+$ HCC cells.

In our study, $CD90^+$ cells expressed the endothelial marker, c-Kit, CD105, and VEGFR1, and a mesenchymal VEC morphology and high metastatic capacity were confirmed in both primary liver cancer and cell lines. We further confirmed that $CD90^+$ liver cancer cells showed chemosensitivity to imatinib mesylate, suggesting that cancer cells committed to mesenchymal endothelial lineages could be eradicated by the compound. Although imatinib mesylate treatment had little effect on the size of primary tumors originated from both $EpCAM^+$ and $CD90^+$ CSCs, it significantly suppressed lung metastasis *in vivo*. These data are consistent with a recent phase II study demonstrating the tolerable toxicity, but limited efficacy, of imatinib mesylate alone for unresectable HCC patients. Eligibility of imatinib mesylate for advanced HCC patients may be restricted to the HCC subtypes organized by $CD90^+$ CSCs with a highly metastatic capacity and VEC features. Therefore, a combination of compounds targeting $EpCAM^+$ tumorigenic CSCs as well as $CD90^+$ metastatic CSCs may be required for the eradication of HCC and should be tested in the future.

Acknowledgments: The authors thank Ms. Nami Nishiyama and Ms. Mikiko Nakamura for their excellent technical assistance.

References

1. Tsai WL, Chung RT. Viral hepatocarcinogenesis. Oncogene 2010;29: 2309-2324.

2. Chiba T, Kita K, Zheng YW, Yokosuka O, Saisho H, Iwama A, et al. Side population purified from hepatocellular carcinoma cells harbors cancer stem cell-like properties. HEPATOLOGY 2006;44:240-251.
3. Haraguchi N, Ishii H, Mimori K, Tanaka F, Ohkuma M, Kim HM, et al. CD13 is a therapeutic target in human liver cancer stem cells. J Clin Invest 2010;120:3326-3339.
4. Ma S, Tang KH, Chan YP, Lee TK, Kwan PS, Castilho A, et al. miR-130b promotes CD133(+) liver tumor-initiating cell growth and self-renewal via tumor protein 53-induced nuclear protein 1. Cell Stem Cell 2010;7:694-707.
5. Yang ZF, Ho DW, Ng MN, Lau CK, Yu WC, Ngai P, et al. Significance of CD90+ cancer stem cells in human liver cancer. Cancer Cell 2008;13:153-166.
6. Zen Y, Fujii T, Yoshikawa S, Takamura H, Tani T, Ohta T, Nakanuma Y. Histological and culture studies with respect to ABCG2 expression support the existence of a cancer cell hierarchy in human hepatocellular carcinoma. Am J Pathol 2007;170:1750-1762.
7. Lee TK, Castilho A, Cheung VC, Tang KH, Ma S, Ng IO. CD24(+) liver tumor-initiating cells drive self-renewal and tumor initiation through STAT3-mediated NANOG regulation. Cell Stem Cell 2011;9: 50-63.
8. Yamashita T, Budhu A, Forgues M, Wang XW. Activation of hepatic stem cell marker EpCAM by Wnt-beta-catenin signaling in hepatocellular carcinoma. Cancer Res 2007;67:10831-10839.
9. Yamashita T, Forgues M, Wang W, Kim JW, Ye Q, Jia H, et al. EpCAM and alpha-fetoprotein expression defines novel prognostic subtypes of hepatocellular carcinoma. Cancer Res 2008;68:1451-1461.
10. Yamashita T, Ji J, Budhu A, Forgues M, Yang W, Wang HY, et al. EpCAM-positive hepatocellular carcinoma cells are tumor-initiating cells with stem/progenitor cell features. Gastroenterology 2009;136: 1012-1024.
11. Ma S, Chan KW, Hu L, Lee TK, Wo JY, Ng IO, et al. Identification and characterization of tumorigenic liver cancer stem/progenitor cells. Gastroenterology 2007;132:2542-2556.
12. Heffelfinger SC, Hawkins HH, Barrish J, Taylor L, Darlington GJ. SK HEP-1: a human cell line of endothelial origin. In Vitro Cell Dev Biol 1992;28A:136-142.
13. Ishimoto T, Nagano O, Yae T, Tamada M, Motohara T, Oshima H, et al. CD44 variant regulates redox status in cancer cells by stabilizing the xCT subunit of system xc(-) and thereby promotes tumor growth. Cancer Cell 2011;19:387-400.
14. Ramadori G, Fuzesi L, Grabbe E, Pieler T, Armbrust T. Successful treatment of hepatocellular carcinoma with the tyrosine kinase inhibitor imatinib in a patient with liver cirrhosis. Anticancer Drugs 2004;15: 405-409.
15. Kim H, Choi GH, Na DC, Ahn EY, Kim GI, Lee JE, et al. Human hepatocellular carcinomas with "Stemness"-related marker expression: keratin 19 expression and a poor prognosis. HEPATOLOGY 2011;54: 1707-1717.
16. Lu JW, Chang JG, Yeh KT, Chen RM, Tsai JJ, Hu RM. Overexpression of Thy1/CD90 in human hepatocellular carcinoma is associated with HBV infection and poor prognosis. Acta Histochem 2011;113: 833-838.
17. Arzumanyan A, Friedman T, Ng IO, Clayton MM, Lian Z, Feitelson MA. Does the hepatitis B antigen HBx promote the appearance of liver cancer stem cells? Cancer Res 2011;71:3701-3708.
18. Yovchev MI, Grozdanov PN, Zhou H, Racherla H, Guha C, Dabeva MD. Identification of adult hepatic progenitor cells capable of repopulating injured rat liver. HEPATOLOGY 2008;47:636-647.
19. Wang Y, Yao HL, Cui CB, Wauthier E, Barbier C, Costello MJ, et al. Paracrine signals from mesenchymal cell populations govern the expansion and differentiation of human hepatic stem cells to adult liver fates. HEPATOLOGY 2010;52:1443-1454.
20. Dome B, Timar J, Ladanyi A, Paku S, Renyi-Vamos F, Klepetko W, et al. Circulating endothelial cells, bone marrow-derived endothelial progenitor cells and proangiogenic hematopoietic cells in cancer: from biology to therapy. Crit Rev Oncol Hematol 2009;69:108-124.
21. Karnoub AE, Dash AB, Vo AP, Sullivan A, Brooks MW, Bell GW, et al. Mesenchymal stem cells within tumour stroma promote breast cancer metastasis. Nature 2007;449:557-563.
22. Mishra PJ, Humeniuk R, Medina DJ, Alexe G, Mesirov JP, Ganesan S, et al. Carcinoma-associated fibroblast-like differentiation of human mesenchymal stem cells. Cancer Res 2008;68:4331-4339.
23. Ricci-Vitiani L, Pallini R, Biffoni M, Todaro M, Invernici G, Cenci T, et al. Tumour vascularization via endothelial differentiation of glioblastoma stem-like cells. Nature 2010;468:824-828.
24. Wang R, Chadalavada K, Wilshire J, Kowalik U, Hovinga KE, Geber A, et al. Glioblastoma stem-like cells give rise to tumour endothelium. Nature 2010;468:829-833.
25. Ho DW, Yang ZF, Yi K, Lam CT, Ng MN, Yu WC, et al. Gene expression profiling of liver cancer stem cells by RNA-sequencing. PLoS One 2012;7:e37159.

J Gastroenterol
DOI 10.1007/s00535-012-0645-5

ORIGINAL ARTICLE—LIVER, PANCREAS, AND BILIARY TRACT

Entecavir and interferon-α sequential therapy in Japanese patients with hepatitis B e antigen-*positive* chronic hepatitis B

Masaru Enomoto · Shuhei Nishiguchi · Akihiro Tamori · Sawako Kobayashi · Hiroki Sakaguchi · Susumu Shiomi · Soo Ryang Kim · Hirayuki Enomoto · Masaki Saito · Hiroyasu Imanishi · Norifumi Kawada

Received: 8 April 2012 / Accepted: 5 July 2012

Abstract
Background The outcomes of sequential therapy with lamivudine followed by interferon have been unsatisfactory in Japanese patients with hepatitis B envelope antigen (HBeAg)-*positive* chronic hepatitis B. However, the efficacy of sequential therapy with entecavir and interferon remains unclear.
Methods Twenty-four HBeAg-*positive* patients (23 men and 1 woman; mean age 39 ± 7 years) received entecavir 0.5 mg alone for 36–52 weeks, followed by entecavir plus interferon-α for 4 weeks, and lastly by interferon-α alone for 20 weeks. Twenty-three patients had genotype C infection, and one had genotype A infection.
Results No entecavir-resistant mutant variants emerged in any patient. Hepatitis flare occurred in three patients during interferon-α treatment after the withdrawal of entecavir, but none had hepatic decompensation. Serum hepatitis B surface antigen levels did not change during or after therapy. Serum hepatitis B core-related antigen levels were significantly decreased at the start ($P < 0.0001$) and at the end of interferon-α treatment ($P < 0.0001$), but returned to baseline levels after treatment. Twenty-four weeks after the completion of the sequential therapy, a sustained biochemical, virological, and serological response was achieved in 5 (21 %) patients. The proportion of patients in whom HBeAg was lost during entecavir treatment was significantly higher among those with a sustained response than among those with no response ($P = 0.015$).
Conclusions The rate of response to sequential therapy with entecavir and interferon-α in Japanese patients with HBeAg-*positive* chronic hepatitis B was not higher than the rate in previous studies of lamivudine followed by interferon.

Keywords Chronic hepatitis B · Genotypes · Interferon-α · Entecavir · Sequential therapy

For the B-SHOT Study Group.
Other members of the B-SHOT Study Group are listed in the Appendix.

M. Enomoto · A. Tamori · S. Kobayashi · H. Sakaguchi · N. Kawada (✉)
Department of Hepatology, Osaka City University Graduate School of Medicine, 1-4-3 Asahimachi, Abeno-ku, Osaka 545-8585, Japan
e-mail: kawadanori@med.osaka-cu.ac.jp

S. Nishiguchi · H. Enomoto · M. Saito · H. Imanishi
Department of Internal Medicine, Hyogo College of Medicine, Hyogo, Japan

S. Shiomi
Department of Nuclear Medicine, Osaka City University Graduate School of Medicine, Osaka, Japan

S. R. Kim
Department of Gastroenterology, Kobe Asahi Hospital, Hyogo, Japan

Introduction

Infection with hepatitis B virus (HBV) remains an important public health problem and a leading cause of liver-related morbidity worldwide [1, 2]. The natural course of chronic HBV infection acquired perinatally or during infancy consists of three distinct phases: 'immune tolerant', 'immune reactive', and 'inactive carrier'. During the immune-reactive phase, rises in alanine aminotransferase (ALT) are attributable to the host's immune response to HBV, and the occurrence of hepatitis will eventually be followed by spontaneous seroconversion from hepatitis B

Published online: 02 August 2012

envelope antigen (HBeAg) to anti-HBe. HBeAg seroconversion usually results in clinical remission and a life-long inactive state; however, patients with persistently detectable HBeAg and high HBV DNA levels who have recurrent hepatitis flares are at increased risk of developing cirrhosis and hepatocellular carcinoma [3, 4].

Currently available antiviral treatment for chronic hepatitis B includes nucleos(t)ide analogues such as lamivudine, adefovir, entecavir, and tenofovir, and the immunomodulator interferon [5–7]. The direct, potent antiviral effects of nucleos(t)ide analogues induce biochemical and virological responses in most patients, but viral relapse and exacerbations of hepatitis commonly occur after discontinuation of treatment. Long-term use of nucleos(t)ide analogues is associated with the emergence of drug-resistant variants possessing mutations in the HBV polymerase gene. In contrast, interferon-induced remission of chronic hepatitis B is durable, but is achieved in only a minority of patients. In randomized controlled trials, concomitant treatment with lamivudine and interferon-α has offered little clinical benefit, in terms of the rates of sustained therapeutic response, as compared with interferon-α alone [8, 9].

Serfaty et al. [10] reported that sequential therapy with lamivudine followed by interferon-α was effective in patients with chronic hepatitis B. In their pilot study in France, sustained virological and biochemical response was achieved in 8 (57 %) of the 14 patients who received lamivudine 100 mg alone for 20 weeks, followed by interferon-α 5 MU 3 times/week plus lamivudine for 4 weeks, and lastly by interferon-α alone for 24 weeks [10]. Some other groups have studied similar protocols for sequential therapy, but results have been conflicting [11–17]. The inconsistent results may have been caused, at least in part, by differences in the included HBV genotypes among studies, because HBV genotypes have specific geographic distributions and can affect the response to interferon [18, 19]. In our previous study [14], the rate of response to sequential therapy with lamivudine and interferon in 24 Japanese HBeAg-*positive* patients with chronic HBV genotype C infection was 29 %, considerably lower than the rate reported by Serfaty et al. [10].

Randomized controlled trials have shown that entecavir has higher antiviral activity against HBV than lamivudine [20, 21]. Among licensed nucleos(t)ide analogues, entecavir is used as a first-line treatment of choice for chronic hepatitis B, similar to tenofovir disoproxil fumarate [22]. Use of a potent nucleoside analogue before the initiation of interferon may improve the outcomes of sequential therapy.

In this study, we evaluated the efficacy of sequential therapy with entecavir and interferon-α in Japanese patients with HBeAg-*positive* chronic hepatitis B. In addition to the monitoring of serum HBeAg and HBV DNA levels, serum hepatitis B surface antigen (HBsAg) and hepatitis B core-related antigen (HBcrAg) [23, 24] levels were monitored during and after sequential therapy. The clinical characteristics of patients who had a sustained response to the sequential therapy were compared with those of patients who had no response.

Patients and methods

Patients

The subjects were 24 Japanese patients with HBeAg-*positive* chronic hepatitis B (23 men and 1 woman; mean age 39 ± 7 years) who had received sequential therapy with entecavir alone and then entecavir plus interferon-α followed by interferon-α alone between September 2006 and August 2011. The inclusion criteria were as follows: (1) persistent or fluctuating elevations of serum ALT levels for at least 6 months before the start of therapy; (2) presence of HBsAg in serum; (3) presence of HBeAg and absence of anti-HBe; (4) presence of HBV DNA $>10^5$ copies/mL (equivalent to 20,000 IU/mL); (5) no use of corticosteroids or immunomodulatory drugs, including interferon, within 1 year before the start of therapy; (6) no use of nucleos(t)ide analogues, such as lamivudine, within 1 year before the start of therapy; (7) absence of resistance to nucleos(t)ide analogues; (8) absence of antibodies to hepatitis C virus and other likely causes of chronic liver disease; and (9) no clinical signs of decompensated cirrhosis or hepatocellular carcinoma. The study procedures were in accordance with the Helsinki Declaration of 1975 (1983 revision) and were approved by the ethics committee of each participating center. Written informed consent was obtained from each patient. This study was registered in the UMIN Clinical Trials Registry (registration ID number, UMIN000000808).

Treatment

Patients were treated with entecavir alone for 36–52 weeks, followed immediately by both entecavir and interferon-α for 4 weeks, and lastly by interferon-α alone for 20 weeks. Entecavir (Baraclude; Bristol-Myers, Tokyo, Japan) was given orally at a dose of 0.5 mg once daily. Natural interferon-α (Otsuka Pharmaceutical, Tokyo, Japan) was given by intramuscular injection, at a dose of 5 MU, three times a week for 24 weeks (a protocol commonly used in Japan during the study period). All patients were followed up for at least 24 weeks after the completion of treatment, and responses to therapy were assessed as follows: *biochemical response* was defined as a decrease in

serum ALT levels to within the normal range; *virological response* was defined as a decrease in serum HBV DNA to $<10^4$ copies/mL; and a *serological response* was defined as loss of serum HBeAg. A sustained response was defined as fulfillment of the criteria for combined biochemical, virological, and serological responses 24 weeks after the end of therapy.

Assays

The following variables were determined for all enrolled patients: complete blood counts; serum ALT level; HBsAg, HBeAg, anti-HBe, HBcrAg, and HBV DNA levels; HBV genotypes; proportion of mutants in the precore and basal core promoter regions of HBV DNA; and drug-resistant mutations in the HBV polymerase gene.

Complete blood counts and serum ALT (upper limit of normal, 30 IU/L) were determined by standard procedures. HBsAg was measured with a chemiluminescent microparticle immunoassay (Architect HBsAg QT; Abbott Japan, Tokyo, Japan) as described elsewhere [25]. HBeAg and anti-HBe were detected with chemiluminescence enzyme immunoassays. HBcrAg was also detected with a chemiluminescence enzyme immunoassay (Fuji-Rebio, Tokyo, Japan) [23]. HBV DNA was measured with a real-time polymerase chain reaction (PCR) assay (COBAS TaqMan HBV Test v2.0; Roche Diagnostics, Tokyo, Japan) [26]. Genotypes of HBV were identified by enzyme-linked immunosorbent assay with monoclonal antibodies to type-specific epitopes in the preS2-region (Institute of Immunology, Tokyo, Japan) [27]. Mutations at nucleotide (*nt*) 1896 in the precore region and at *nt* 1762 and *nt* 1764 in the basal core promoter region of HBV DNA were found by means of an enzyme-linked minisequence assay (Genome Science Laboratory, Tokyo, Japan). Drug-resistant mutations (at codons 180, 181, 184, 202, 204, 236, and 250 of the HBV reverse transcriptase domain) were detected by PCR-Invader technology (BML, Tokyo, Japan) [28].

Histopathology

When informed consent had been obtained, a liver biopsy was performed before the patient started therapy. Histopathological findings were assessed by grading inflammatory activity and staging fibrosis according to the METAVIR scoring system [29]. An experienced pathologist blinded to the clinical data performed these evaluations.

Statistical analysis

Statistical analysis was performed with SAS, version 9.2 for Windows (SAS Institute, Cary, NC, USA). Distributions of continuous variables were analyzed with the non-parametric Mann–Whitney *U*-test. Differences in proportions were tested by Fisher's exact test. The significance of changes in values between two time points was evaluated by the Wilcoxon signed-rank test. A two-tailed *P* value of less than 0.05 was considered to indicate statistical significance.

Results

Rate of response to therapy

Although common interferon-α-related side effects included pyrexia, fatigue, headache, and myalgia, the therapy was well tolerated, and all patients completed the treatment according to the protocol. The proportions of patients with biochemical, virological, and serological responses during and after sequential therapy with entecavir and interferon-α are shown in Fig. 1. Drug-resistant mutant variants did not emerge in any patient during entecavir treatment. At the start of interferon-α treatment (about 1 year after the start of the entecavir treatment), most patients had normal ALT levels and serum HBV DNA levels of $<10^4$ copies/mL

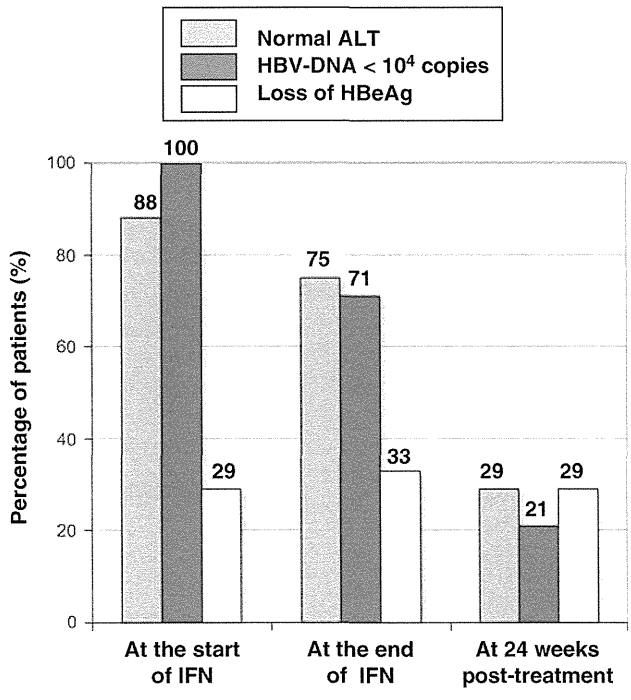

Fig. 1 Rate of biochemical, virological, and serological responses during and after sequential therapy with entecavir and interferon-α. Combined sustained biochemical, virological, and serological response was achieved in 5 (21 %) of the 24 enrolled patients 24 weeks after completion of the sequential therapy. *ALT* Alanine aminotransferase, *HBeAg* hepatitis B envelope antigen, *HBV* hepatitis B virus, *IFN* interferon

(88 and 100 %, respectively). However, loss of HBeAg was achieved in a minority of patients (29 %) during the entecavir treatment.

In most patients without HBeAg loss at the end of the entecavir treatment, serum ALT and HBV DNA levels increased even during the interferon-α treatment. Hepatitis flare (defined as a rise in ALT equivalent to 10 times higher than the upper limit of normal and more than twice the baseline value) occurred in 3 patients after the withdrawal of entecavir. Although peak ALT levels in these patients were 693, 721, and 876 IU/L, respectively, none had jaundice or hepatic decompensation. At the end of the interferon-α treatment, the percentages of patients with normal ALT, HBV DNA $<10^4$ copies/mL, and loss of HBeAg were 75, 71, and 33 %, respectively.

Lastly, 24 weeks after the completion of the sequential therapy, a sustained biochemical, virological, and serological response was achieved in 5 (21 %) of the 24 patients. No patient had loss of serum HBsAg in response to the sequential therapy.

Changes in HBsAg and HBcrAg during and after sequential therapy

Changes in serum HBsAg and HBcrAg levels during and after the sequential therapy with entecavir and interferon-α are shown in Fig. 2. The serum HBsAg level did not change significantly during or after the therapy (Fig. 2a). The serum HBcrAg levels were significantly decreased at the start ($P < 0.0001$) and at the end of interferon-α treatment ($P < 0.0001$), but returned to baseline levels after completion of the sequential treatment (Fig. 2b). The serum HBsAg level did not differ significantly between patients with a sustained response and those with no response (Fig. 2c). In contrast, the serum HBcrAg level was significantly lower in patients with a sustained response than in those with no response at the end of the interferon-α therapy ($P = 0.013$) and 24 weeks post-treatment ($P = 0.031$) (Fig. 2d).

Characteristics of patients at the start of entecavir treatment

The baseline demographic, biochemical, virological, and histological characteristics of patients at the start of entecavir treatment, classified according to the response to sequential therapy, are listed in Table 1. The mean age of patients with a sustained response was more than 10 years less than that of the patients with no response, but this difference did not reach statistical significance ($P = 0.102$). There were no significant differences between the two groups with respect to sex ratio, proportion of patients with a history of interferon treatment, ALT level, HBV DNA level, ratios of HBV genotypes, ratios of precore or basal core promoter mutants, or histopathological findings in the liver.

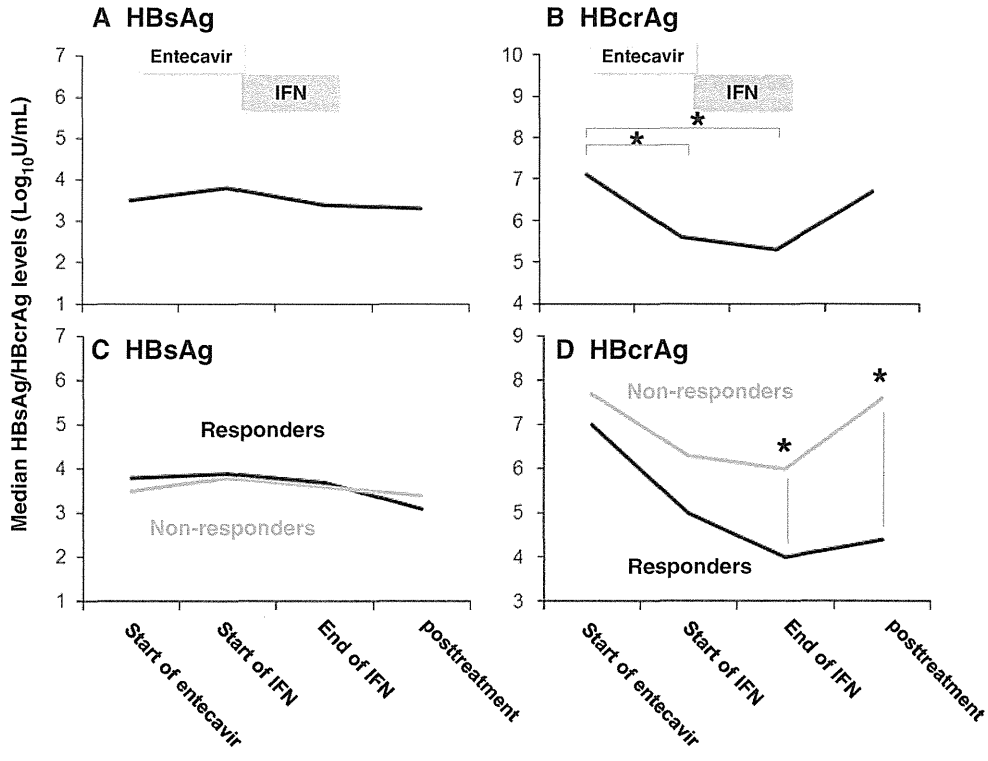

Fig. 2 Changes in serum levels of hepatitis B surface antigen (*HBsAg*) and hepatitis B core-related antigen (*HBcrAg*) during and after sequential therapy with entecavir and interferon-α. Serum HBsAg levels did not change during or after therapy (**a**). As compared with the baseline value, the serum HBcrAg level was significantly decreased at the start ($P < 0.0001$) and at the end of interferon-α treatment ($P < 0.0001$) (*asterisks*) (**b**). When sustained responders were compared with non-responders, there was no significant difference in the serum HBsAg level (**c**). In contrast, the serum HBcrAg level was significantly lower in sustained responders than in non-responders at the end of interferon-α therapy ($P = 0.013$) and 24 weeks post-treatment ($P = 0.031$) (*asterisks*) (**d**)

Table 1 Baseline characteristics of patients at the start of entecavir treatment

Characteristics	Sustained responders ($n = 5$)	Non-responders ($n = 19$)	P values
Age (years)	29 ± 6	41 ± 5	0.10
Male sex (%)	5 (100 %)	18 (95 %)	0.99
History of interferon treatment (%)	3 (60 %)	12 (63 %)	0.99
ALT (IU/L)	85 (65, 322)	210 (79, 531)	0.37
HBV DNA ($\log_{10}$ copies/mL)	7.7 ± 0.4	7.8 ± 0.8	0.31
Genotype (A/B/C/D)	0/0/5/0	1/0/18/0	0.99
Precore (wild/mixed/mutant)	0/4/1	9/9/1	0.12
Basal core promoter (wild/mixed/mutant)	1/0/4	5/8/6	0.070
Grade of inflammation (mild/moderate/severe)	2/3/0	9/7/2	0.60
Stage of fibrosis (mild/moderate/severe/cirrhosis)	2/2/0/1	10/5/3/0	0.19

Values are means ± SDs for normally distributed variables, and medians (with the interquartile range) for non-normally distributed variables

ALT alanine aminotransferase, *HBV* hepatitis B virus

Table 2 Characteristics of patients at the start of interferon-α treatment

Characteristics	Sustained responders ($n = 5$)	Non-responders ($n = 19$)	P values
ALT (IU/L)	24 (23, 35)	20 (15, 32)	0.27
ALT normal (%)	5 (100 %)	16 (84 %)	0.99
HBV DNA ($\log_{10}$ copies/mL)	2.1 ± 0.3	2.3 ± 0.4	0.18
HBV DNA negative (%)	3 (60 %)	6 (32 %)	0.33
HBeAg loss (%)	4 (80 %)	3 (16 %)	0.015

Values are means ± SDs for normally distributed variables, and medians (with the interquartile range) for non-normally distributed variables

HBeAg hepatitis B envelope antigen

Characteristics of patients at the start of interferon-α treatment

The characteristics of the patients at the start of interferon-α treatment, classified according to the response to sequential therapy, are shown in Table 2. The responders and non-responders did not differ significantly with respect to ALT level or HBV DNA level at the start of interferon-α treatment. The proportion of patients in whom HBeAg was lost during entecavir treatment was significantly higher among those with a sustained response than among those with no response ($P = 0.015$). In another comparison, a sustained response was achieved in 4 (57 %) of the 7 patients with loss of HBeAg during entecavir treatment, as compared with 1 (5.9 %) of the 17 patients without loss of HBeAg during treatment; this difference was also statistically significant ($P = 0.015$).

Case presentation

A 24-year-old man with no response to previous treatment with interferon-α was referred to us (Fig. 3). His ALT level

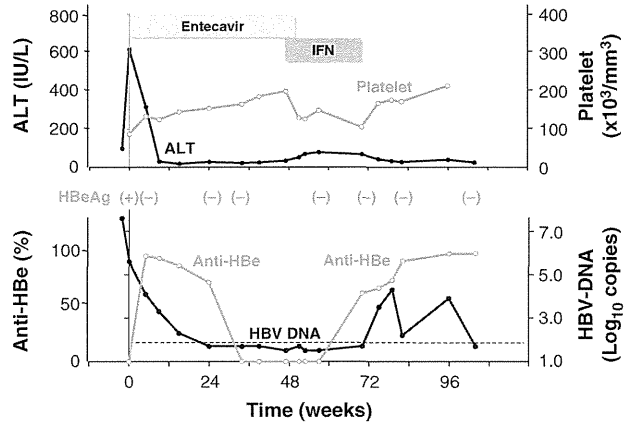

Fig. 3 Changes in platelet count, ALT, HBeAg, anti-HBe, and HBV DNA in a 24-year-old man with sustained response to sequential therapy with entecavir and interferon-α. In the *upper panel*, the changes in ALT levels (*filled circles*) and platelet counts (*open circles*) are shown. In the *lower panel*, the changes in HBV DNA (*filled circles*) and anti-HBe (*open circles*) titers are shown. During 1 year of entecavir treatment, the platelet count rose from 87,000 to 199,000/mm^3. After the patient was switched to interferon-α, his anti-HBe antibody titer increased. At the most recent hospital visit, the patient's ALT level was normal, HBeAg was negative, and HBV DNA was negative; the patient has remained drug-free since the completion of treatment

was 617 IU/L, HBV DNA level was 7.6 $\log_{10}$ copies/mL, and HBV genotype was C. A precore stop codon mutation at *nt* 1896 and basal core promoter mutations at *nt* 1762 and *nt* 1764 were detected. A liver biopsy showed moderate inflammation and cirrhosis. Although the patient was young, interferon-α was not indicated because of a low platelet count and concern about exacerbation of hepatitis. However, during 1 year of entecavir treatment, his ALT level became normal, and his platelet count rose from 87,000 to 199,000/mm^3. After switching to interferon-α, his HBV DNA rose transiently, but his anti-HBe antibody titer increased. At the most recent hospital visit (up to 35 weeks after the completion of treatment), his ALT level was normal and HBeAg and HBV DNA were negative; the

patient has remained drug-free since the completion of treatment.

Discussion

Several groups have evaluated protocols for sequential therapy with lamivudine and interferon-α, and their protocols were similar to that originally described by Serfaty et al. [10]. Manesis et al. [11], from Greece, where HBV genotype D is predominant, found that in HBeAg-*negative* patients, the rate of sustained biochemical and virological response was 22 %, which did not differ from that obtained in an age/sex-matched historical control group treated with interferon-α alone. In another report from Greece [12], sequential combination therapy significantly prevented the emergence of resistance to lamivudine, but the rate of sustained virological response was only 17 % among HBeAg-*negative* patients. A group from China, where genotype B or C is predominant, reported very similar results [13]. To date, only the study by Moucari et al. [17] has used adefovir dipivoxil instead of lamivudine. Sustained virological response was achieved in 50 % of their subjects, although only 20 HBeAg-*negative* patients were included.

In Japan and other countries in East Asia, genotype C is the most prevalent type of HBV [18, 19], and most patients with chronic hepatitis B acquire the virus perinatally or in early childhood [7]. The rates of response to interferon are thus lower than those reported in Europe and the United States. In our previous study [14], using a sequential therapy protocol similar to that described by Serfaty et al. [10], we found that the rate of sustained response was only 29 % among 24 HBeAg-*positive* patients. The patients with a sustained response were significantly younger and had a significantly lower HBV DNA level at the start of interferon than did those with no response. The rate of HBeAg loss during lamivudine treatment was slightly but not significantly higher among sustained responders than among non-responders. Minami and Okanoue [15] also found that patients who lost HBeAg during lamivudine treatment were more likely to have a sustained response to sequential therapy. Okuse et al. [16] reported that sequential therapy was effective for patients with acute exacerbations of chronic hepatitis B, particularly those in whom HBeAg had become negative during lamivudine treatment.

One objective of sequential therapy is to lower the viral load by the use of a nucleos(t)ide analogue, thereby restoring sensitivity to interferon treatment. In clinical studies, a low HBV DNA level is predictive of a favorable response to interferon-α [30, 31]. In basic studies, a high viral load is associated with T-cell hyporesponsiveness [32], and treatment with nucleos(t)ide analogues restores cellular immune response in chronic HBV infection [33]. Although lamivudine had been administered for about half a year before the start of interferon administration in previous studies (including ours) [10–16], we administered entecavir, a more potent antiviral agent, for about 1 year in the present study. Treatment with entecavir was given for a longer period because it has been reported in previous studies that patients in whom HBeAg and HBV DNA levels were lowered by lamivudine were more likely to have a sustained response and because few entecavir-resistant variants emerge within the first few years [34]. However, the use of entecavir for a longer duration did not raise the rate of off-treatment sustained response to sequential therapy in the present study, although the rate of on-treatment biochemical and virological responses was higher with entecavir than that obtained with lamivudine in our previous study [14].

Another objective of sequential therapy is to prevent the relapse of hepatitis after discontinuation of the nucleos(t)ide analogue through the use of interferon-α. Nucleos(t)ide analogues rapidly decrease serum HBV DNA levels by suppressing the reverse transcription of pregenomic HBV RNA, but viral relapse commonly occurs after the cessation of treatment. This high risk of viral relapse may be attributed to the persistence of HBV replicative intermediate covalently closed circular DNA (cccDNA) in the liver even during nucleos(t)ide treatment. The measurement of HBV antigens in serum is thus clinically important as a surrogate marker of intrahepatic cccDNA. In particular, a decline in serum levels of HBsAg is strongly associated with response to interferon-α [35]. The HBcrAg assay measures serum levels of all antigens transcribed from the precore/core gene, including hepatitis B core and e antigens, by using monoclonal antibodies that recognize common epitopes of the denatured antigens [23, 24]. Matsumoto et al. [36] recently proposed a model for predicting relapse of hepatitis after discontinuation of nucleos(t)ide analogue administration, in which cut-off values were set at 1.9–2.9 $\log_{10}$ IU/mL of HBsAg and 3.0–4.0 $\log_{10}$ U/mL of HBcrAg at the withdrawal of treatment. In our study, only one patient had a decrease in HBsAg to between 1.9 and 2.9 $\log_{10}$ IU/mL and another one had a decrease in HBcrAg to between 3.0 and 4.0 $\log_{10}$ U/mL at the withdrawal of entecavir (data not shown), probably because of an insufficient duration of entecavir treatment in our protocol. The finding that at least 21 % of our patients with insufficient HBsAg and HBcrAg decline during entecavir treatment achieved a sustained response to sequential therapy suggests that switching to interferon-α contributes to the safe termination of nucleos(t)ide analogue treatment in some patients.

The major advantages of interferon-α include a finite course of treatment, the opportunity to obtain an off-treatment durable response to therapy, and absence of drug resistance. The advantages of nucleos(t)ide analogues include good tolerance and potent antiviral activity associated with high rates of on-treatment response to therapy. Guidelines proposed by the Japanese Study Group of the Standardization of Treatment of Viral Hepatitis basically recommend interferon-α as the first-line treatment for patients with chronic hepatitis B who are younger than 35 years, to attain a 'drug-free state'; and entecavir for patients who are 35 years or older, to persistently suppress HBV DNA [37]. Consistent with the findings of previous studies [14–16], our results show that sequential therapy is best indicated for patients who have lost HBeAg during nucleoside analogue treatment, because such patients have a higher probability of a sustained response. As shown in Fig. 3, patients who are young but have exacerbation of hepatitis, cirrhosis, or both, were also good candidates for sequential therapy, because interferon-α is generally not recommended for such patients because of concern about hepatic decompensation, and the preceding use of a nucleos(t)ide analogue can reduce such risk.

Our study had several limitations. First, it was not a randomized controlled trial. The reported rate of HBeAg seroconversion obtained by 6-month interferon-α monotherapy among Japanese patients was about 20 % [38], which is similar to the rate obtained by the sequential therapy used in our study (21 %). As compared with our previous study of lamivudine [14], the rate of sustained response in our present study of entecavir did not differ significantly (21 % in the entecavir group vs. 29 % in the lamivudine group). Although the patients were not randomly assigned to treatment, the baseline characteristics of the subjects did not differ between those in our previous study of lamivudine and those in the present study of entecavir with respect to mean age, sex ratio, ALT level, HBV DNA level, ratios of HBV genotypes, ratios of precore or basal core promoter mutants, or histopathological findings (data not shown). Thus, we cannot conclude that sequential therapy with entecavir and interferon-α is more effective than interferon-α monotherapy or sequential therapy with lamivudine and interferon-α. Second, we gave patients non-pegylated interferon-α for 6 months, because pegylated interferon-α had not been approved for the treatment of chronic hepatitis B by the Japanese medical insurance system during the study period. Further studies are thus needed to evaluate the efficacy of sequential therapy with entecavir and pegylated interferon-α.

To our knowledge, this is the first study to report on the response to sequential therapy with entecavir and interferon-α in patients with chronic hepatitis B. In summary, an off-treatment sustained response to sequential therapy with entecavir and interferon-α was achieved in 21 % of HBeAg-*positive* patients with chronic hepatitis B in Japan, where genotype C is predominant. This rate of response was not higher than that in our previous study using lamivudine [14]. Patients who had loss of HBeAg during entecavir treatment were more likely to have a sustained response to sequential therapy.

Acknowledgments The authors are grateful to Ms. Sanae Deguchi, Ms. Rie Yasuda, and Ms. Ami Saito for their technical assistance. This work was supported in part by a grant from the Ministry of Health, Labour and Welfare, Japan.

Conflict of interest Dr. Shuhei Nishiguchi has received research grants from Bristol-Myers K.K. and Otsuka Pharmaceutical Co., Ltd. Dr. Norifumi Kawada has received research grants from Bristol-Myers K.K. and Otsuka Pharmaceutical Co., Ltd.

Appendix

In addition to the authors, the B-SHOT Study Group includes the following persons: Kohshun Kim, Motoharu Tanaka (Higashi Sumiyoshi Morimoto Hospital, Osaka, Japan); Hideji Nakamura, Hiroko Iijima, Soji Shimomura, Noritoshi Koh, Yoshinori Iwata, Yoshiyuki Sakai, Tomoyuki Takashima (Hyogo College of Medicine, Nishinomiya, Japan); Tetsuo Yamamoto (Kita-Osaka Police Hospital, Osaka); Hirokazu Kadoya (Izumiotsu Municipal Hospital, Osaka); Chika Kawamura (Ohno Memorial Hospital, Osaka); Kiyohide Kioka, Yasuko Kawasaki (Osaka City General Hospital, Osaka); Osamu Kurai, Hiroko Oka (Osaka City Juso Hospital, Osaka); Daiki Habu, Hiroyasu Morikawa, Shuji Iwai, Hideki Fujii (Osaka City University Medical School, Osaka); Katsuhiko Fukuda (PL Hospital, Osaka); Machiko Shintani (Sumiyoshi Municipal Hospital, Osaka); and Hisato Jomura (Wakakokai Hospital, Osaka).

References

1. Dienstag JL. Hepatitis B virus infection. N Engl J Med. 2008;359:1486–500.
2. Liaw YF, Chu CM. Hepatitis B virus infection. Lancet. 2009;373:582–92.
3. Iloeje U, Yang H, Su J, Jen CL, You SL, Chen CJ. Predicting cirrhosis risk based on the level of circulating hepatitis B viral load. Gastroenterology. 2006;130:678–86.
4. Chen CJ, Yang HI, Su J, Jen CL, You SL, Lu SN, et al. Risk of hepatocellular carcinoma across a biological gradient of serum hepatitis B virus DNA level. JAMA. 2006;295:65–73.
5. Lok AS, McMahon BJ. Chronic hepatitis B: update 2009. Hepatology. 2009;50:661–2.

6. European Association For The Study Of The Liver. EASL Clinical Practice Guidelines: management of chronic hepatitis B. J Hepatol. 2009;50:227–42.
7. Liaw YF, Leung N, Kao JH, Piratvisuth T, Gane E, Han KH, et al. Asian-Pacific consensus statement on the management of chronic hepatitis B: a 2008 update. Hepatol Int. 2008;2:263–83.
8. Janssen HL, van Zonneveld M, Senturk H, Zeuzem S, Akarca US, Cakaloglu Y, et al. Pegylated interferon alfa-2b alone or in combination with lamivudine for HBeAg-positive chronic hepatitis B: a randomised trial. Lancet. 2005;365:123–9.
9. Lau GK, Piratvisuth T, Luo KX, Marcellin P, Thongsawat S, Cooksley G, et al. Peginterferon Alfa-2a, lamivudine, and the combination for HBeAg-positive chronic hepatitis B. N Engl J Med. 2005;352:2682–95.
10. Serfaty L, Thabut D, Zoulim F, Andreani T, Chazouillères O, Carbonell N, et al. Sequential treatment with lamivudine and interferon monotherapies in patients with chronic hepatitis B not responding to interferon alone: results of a pilot study. Hepatology. 2001;34:573–7.
11. Manesis EK, Papatheodoridis GV, Hadziyannis SJ. A partially overlapping treatment course with lamivudine and interferon in hepatitis B e antigen-negative chronic hepatitis B. Aliment Pharmacol Ther. 2006;23:99–106.
12. Vassiliadis T, Tziomalos K, Patsiaoura K, Zagris T, Giouleme O, Soufleris K, et al. Lamivudine/pegylated interferon alfa-2b sequential combination therapy compared with lamivudine monotherapy in HBeAg-negative chronic hepatitis B. J Gastroenterol Hepatol. 2007;22:1582–8.
13. Shi M, Wang RS, Zhang H, Zhu YF, Han B, Zhang Y, et al. Sequential treatment with lamivudine and interferon-alpha monotherapies in hepatitis B e antigen-negative Chinese patients and its suppression of lamivudine-resistant mutations. J Antimicrob Chemother. 2006;58:1031–5.
14. Enomoto M, Tamori A, Kohmoto MT, Hayashi T, Morikawa H, Jomura H, et al. Lamivudine and IFN-beta sequential therapy in HBe antigen-positive patients with chronic hepatitis B virus genotype C infection. J Interferon Cytokine Res. 2007;27:201–7.
15. Minami M, Okanoue T. Management of HBV infection in Japan. Hepatol Res 2007; 37(s1):S79–82.
16. Okuse C, Yotsuyanagi H, Yamada N, Okamoto M, Ikeda H, Kobayashi M, et al. Effect of nucleoside analog-interferon sequential therapy on patients with acute exacerbation of chronic hepatitis B. Hepatol Res. 2010;40:461–9.
17. Moucari R, Boyer N, Ripault MP, Castelnau C, Mackiewicz V, Dauvergne A, et al. Sequential therapy with adefovir dipivoxil and pegylated Interferon Alfa-2a for HBeAg-negative patients. J Viral Hepat. 2011;18:580–6.
18. Orito E, Ichida T, Sakugawa H, Sata M, Horiike N, Hino K, et al. Geographic distribution of hepatitis B virus (HBV) genotype in patients with chronic HBV infection in Japan. Hepatology. 2001; 34:590–4.
19. Enomoto M, Tamori A, Nishiguchi S. Hepatitis B virus genotypes and response to antiviral therapy. Clin Lab. 2006;52:43–7.
20. Chang TT, Gish RG, de Man R, Gadano A, Sollano J, Chao YC, et al. A comparison of entecavir and lamivudine for HBeAg-positive chronic hepatitis B. N Engl J Med. 2006;354:1001–10.
21. Lai CL, Shouval D, Lok AS, Chang TT, Cheinquer H, Goodman Z, et al. Entecavir versus lamivudine for patients with HBeAg-negative chronic hepatitis B. N Engl J Med. 2006;354:1011–20.
22. Marcellin P, Heathcote EJ, Buti M, Gane E, de Man RA, Krastev Z, et al. Tenofovir disoproxil fumarate versus adefovir dipivoxil for chronic hepatitis B. N Engl J Med. 2008;359:2442–55.
23. Kimura T, Rokuhara A, Sakamoto Y, Yagi S, Tanaka E, Kiyosawa K, et al. Sensitive enzyme immunoassay for hepatitis B virus core-related antigens and their correlation to virus load. J Clin Microbiol. 2002;40:439–45.
24. Rokuhara A, Tanaka E, Matsumoto A, Kimura T, Yamaura T, Orii K, et al. Clinical evaluation of a new enzyme immunoassay for hepatitis B virus core-related antigen; a marker distinct from viral DNA for monitoring lamivudine treatment. J Viral Hepat. 2003;10:324–30.
25. Kohmoto M, Enomoto M, Tamori A, Habu D, Takeda T, Kawada N, et al. Quantitative detection of hepatitis B surface antigen by chemiluminescent microparticle immunoassay during lamivudine treatment of chronic hepatitis B virus carriers. J Med Virol. 2005;75:235–9.
26. Hochberger S, Althof D. Gallegos de Schrott R, Nachbaur N, Röck H, Leying H. Fully automated quantitation of hepatitis B virus (HBV) DNA in human plasma by the COBAS AmpliPrep/ COBAS TaqMan system. J Clin Virol. 2006;35:373–80.
27. Usuda S, Okamoto H, Iwanari H, Baba K, Tsuda F, Miyakawa Y, et al. Serological detection of hepatitis B virus genotypes by ELISA with monoclonal antibodies to type-specific epitopes in the preS2-region product. J Virol Methods. 1999;80:97–112.
28. Tadokoro K, Suzuki F, Kobayashi M, Yamaguchi T, Nagano M, Egashira T, et al. Rapid detection of drug-resistant mutations in hepatitis B virus by the PCR-Invader assay. J Virol Methods. 2011;171:67–73.
29. Bedossa P, Poynard T. An algorithm for the grading of activity in chronic hepatitis C. The METAVIR Cooperative Study Group. Hepatology. 1996;24:289–93.
30. Perrillo RP, Schiff ER, Davis GL, Bodenheimer HC Jr. Lindsay K, Payne J, et al. A randomized, controlled trial of interferon alfa-2b alone and after prednisone withdrawal for the treatment of chronic hepatitis B. The Hepatitis Interventional Therapy Group. N Engl J Med. 1990;323:295–301.
31. Lok AS, Wu PC, Lai CL, Lau JY, Leung EK, Wong LS, et al. A controlled trial of interferon with or without prednisone priming for chronic hepatitis B. Gastroenterology. 1992;102:2091–7.
32. Chisari FV, Ferrari C. Hepatitis B virus immunopathogenesis. Annu Rev Immunol. 1995;13:29–60.
33. Boni C, Bertoletti A, Penna A, Cavalli A, Pilli M, Urbani S, et al. Lamivudine treatment can restore T cell responsiveness in chronic hepatitis B. J Clin Invest. 1998;102:968–75.
34. Tenney DJ, Rose RE, Baldick CJ, Pokornowski KA, Eggers BJ, Fang J, et al. Long-term monitoring shows hepatitis B virus resistance to entecavir in nucleoside-naïve patients is rare through 5 years of therapy. Hepatology. 2009;49:1503–14.
35. Sonneveld MJ, Rijckborst V, Boucher CA, Hansen BE, Janssen HL. Prediction of sustained response to peginterferon alfa-2b for hepatitis B e antigen-positive chronic hepatitis B using on-treatment hepatitis B surface antigen decline. Hepatology. 2010;52: 1251–7.
36. Matsumoto A, Tanaka E, Suzuki Y, Kobayashi M, Tanaka Y, Shinkai N, et al. Combination of hepatitis B viral antigens and DNA for prediction of relapse after discontinuation of nucleos(t)ide analogs in patients with chronic hepatitis B. Hepatol Res. 2012;42:139–49.
37. Kumada H, Okanoue T, Onji M, Moriwaki H, Izumi N, Tanaka E, et al. Guidelines for the treatment of chronic hepatitis and cirrhosis due to hepatitis B virus infection for the fiscal year 2008 in Japan. Hepatol Res. 2010;40:1–7.
38. Suzuki F, Arase Y, Akuta N, Tsubota A, Suzuki Y, Sezaki H, et al. Efficacy of 6-month interferon therapy in chronic hepatitis B virus infection in Japan. J Gastroenterol. 2004;39:969–74.